

1                   **Impact of dust addition on Mediterranean plankton**  
2                   **communities under present and future conditions of pH and**  
3                   **temperature: an experimental overview**

4 Frédéric Gazeau<sup>1</sup>, Céline Ridame<sup>2</sup>, France Van Wambeke<sup>3</sup>, Samir Alliouane<sup>1</sup>, Christian Stolpe<sup>1</sup>,  
5 Jean-Olivier Irisson<sup>1</sup>, Sophie Marro<sup>1</sup>, Jean-Michel Grisoni<sup>4</sup>, Guillaume De Liège<sup>4</sup>, Sandra  
6 Nunige<sup>3</sup>, Kahina Djaoudi<sup>3</sup>, Elvira Pulido-Villena<sup>3</sup>, Julie Dinasquet<sup>5,6</sup>, Ingrid Obernosterer<sup>6</sup>,  
7 Philippe Catala<sup>6</sup>, Cécile Guieu<sup>1</sup>

8 <sup>1</sup> Sorbonne Université, CNRS, Laboratoire d'Océanographie de Villefranche, LOV, 06230  
9 Villefranche-sur-Mer, France

10 <sup>2</sup> CNRS-INSU/IRD/MNHN/UPMC, LOCEAN: Laboratoire d'Océanographie et du Climat:  
11 Expérimentation et Approches Numériques, UMR 7159, 75252 Paris Cedex 05, France

12 <sup>3</sup> Aix-Marseille Université, Université de Toulon, CNRS/INSU, IRD, MIO, UM 110, 13288,  
13 Marseille, France

14 <sup>4</sup> Sorbonne Université, CNRS, Institut de la Mer de Villefranche, IMEV, 06230 Villefranche-sur-  
15 Mer, France

16 <sup>5</sup> Scripps Institution of Oceanography, University of California San Diego, USA

17 <sup>6</sup> CNRS, Sorbonne Université, Laboratoire d'Océanographie Microbienne, LOMIC, F-66650  
18 Banyuls-sur-Mer, France

19 Correspondence to: Frédéric Gazeau ([f.gazeau@obs-vlfr.fr](mailto:f.gazeau@obs-vlfr.fr))

20 Keywords: Mediterranean Sea; Atmospheric deposition; Plankton community; Ocean  
21 acidification; Ocean warming

## 22 Abstract

23 In Low Nutrient Low Chlorophyll areas, such as the Mediterranean Sea, atmospheric  
24 fluxes represent a considerable external source of nutrients likely ~~supporting primary production~~  
25 especially during ~~stratification~~ periods. These areas are expected to expand in the future due to  
26 lower nutrient supply from sub-surface waters caused by climate-driven enhanced stratification,  
27 ~~likely~~ further increasing the ~~role~~ of atmospheric deposition as a source of new nutrients to  
28 surface waters. ~~Yet~~, whether plankton communities will react differently to dust deposition in a  
29 warmer and acidified environment remains an open question. The potential impact of dust  
30 deposition both in present and future ~~climate~~ conditions was investigated ~~through~~ three  
31 ~~perturbation~~ experiments in the open Mediterranean Sea. Climate reactors (300 L) were filled  
32 with surface water collected in the Tyrrhenian Sea, Ionian Sea and in the Algerian basin during a  
33 cruise conducted ~~in May/June 2017~~ in the frame of the PEACETIME project. The ~~experimental~~  
34 ~~protocol~~ comprised two unmodified control tanks, two tanks enriched with a Saharan dust analog  
35 and two tanks enriched with the dust analog and maintained under warmer (+3 °C) and acidified  
36 (-0.3 pH unit) conditions. Samples for the analysis of an extensive number of biogeochemical  
37 parameters and processes were taken over the duration of ~~the~~ experiments (3-4 d). ~~Here, we~~  
38 ~~present the general setup of the experiments and the impacts of dust seeding with and without~~  
39 ~~addressing the effects of environmental changes on nutrients and biological stocks.~~ Dust addition  
40 led to a rapid ~~and maximum input of nitrate whereas phosphate~~ release from the dust analog ~~was~~  
41 ~~much smaller~~. Our results showed that the impacts of Saharan dust deposition in three different  
42 basins of the open Northwestern Mediterranean Sea are at least as strong as those observed  
43 previously in coastal waters. ~~However, interestingly~~, the effects of dust deposition on biological  
44 ~~stocks~~ were ~~highly~~ different ~~between~~ the three investigated stations and could not be attributed to  
45 differences in their degree of oligotrophy but rather to the initial metabolic state of the  
46 community. Ocean acidification and warming did not drastically modify the composition of the

47 autotrophic assemblage with all groups positively impacted by warming and acidification.  
48 ~~Although autotrophic biomass was more positively impacted than heterotrophic biomass~~ under  
49 future environmental conditions, a stronger impact of warming and acidification on  
50 mineralization processes suggests a decreased capacity of Mediterranean surface plankton  
51 communities to sequester atmospheric CO<sub>2</sub> following the deposition of atmospheric particles.

## 52 1. Introduction

53 Atmospheric deposition is well recognized as a significant source of micro- and macro-  
54 nutrients for surface waters of the global ocean (Duce et al., 1991; Jickells et al., 2005; Moore et  
55 al., 2013). The potential modulation of the biological carbon pump efficiency and the associated  
56 export of carbon by atmospheric deposition events are still poorly understood and quantified  
57 (Law et al., 2013). This is especially true for Low Nutrient Low Chlorophyll (LNLC) areas  
58 where atmospheric fluxes can play a considerable role in nutrient cycling and that represent 60%  
59 of the global ocean surface area (Longhurst et al., 1995) as well as 50% of global carbon export  
60 (Emerson et al., 1997). These regions are characterized by ~~a~~ low availability of macronutrients  
61 (N, P) and ~~or metal~~ micronutrients (e.g. Fe) that can severely limit or co-limit phytoplankton  
62 growth during large periods of year.

63 The Mediterranean Sea is a typical example of these LNLC regions ~~and exhibits~~ surface  
64 chlorophyll *a* concentrations below 0.2  $\mu\text{g L}^{-1}$  all year round ~~over most of its area~~, except in the  
65 Ligurian Sea where relatively large blooms can be observed in late winter-early spring (e.g.  
66 Mayot et al., 2016). Recent ~~assessments showed~~ that the atmospheric input of nutrients in the  
67 Mediterranean Sea is ~~of~~ the same order of magnitude as riverine inputs (Powley et al., 2017),  
68 ~~making the atmosphere a considerable external~~ source of nutrients (Richon et al., 2018).

69 Atmospheric deposition originates both from natural (mainly Saharan dust) and anthropogenic  
70 sources (e.g. Bergametti et al., 1989; Desboeufs et al., 2018). Dust deposition, mostly in the form  
71 of pulsed inputs, is mainly associated with wet deposition (Loÿe-Pilot and Martin, 1996). Ternon  
72 et al. (2010) reported an average annual dust flux over four years of 11.4  $\text{g m}^{-2} \text{yr}^{-1}$  (average  
73 during the period 2003–2007) at the DYFAMED station in the Northwestern Mediterranean Sea.  
74 In this region, the most important events reported in the ~~2010~~ decade amounted to  $\sim 22 \text{ g m}^{-2}$   
75 (Bonnet and Guieu, 2006; Guieu et al., 2010b).

76 Atmospheric deposition provides new nutrients to ~~the~~ surface waters (Guieu et al., 2010b;  
77 Kouvarakis et al., 2001; Markaki et al., 2003; Ridame and Guieu, 2002), ~~Fe~~ (Bonnet and Guieu,  
78 2006) ~~and other trace metals~~ (Desboeufs et al., 2018; Guieu et al., 2010b; Theodosi et al., 2010),  
79 ~~that represent~~ significant inputs likely supporting ~~the~~ primary production ~~especially~~ during the  
80 stratification ~~period~~ (Bonnet et al., 2005; Ridame and Guieu, 2002), although no ~~clear~~ correlation  
81 between dust and ~~ocean color could be evidenced from long series of satellite observation in that~~  
82 ~~part of the basin~~ (Guieu and Ridame, 2020).

83 ~~Experimental approaches~~ have shown that wet dust deposition events in the Northwestern  
84 Mediterranean Sea (the dominant deposition mode in that basin) ~~present a higher impact as a~~  
85 source of bioavailable ~~fertilizing~~ nutrients compared to dry deposition. ~~Indeed,~~ wet deposition  
86 provides both new N and P while dry deposition supplies ~~only~~ P and does not ~~allow to~~ stimulate  
87 ~~the autotrophic community (except diazotrophs;~~ Ridame et al., 2013), resulting in no ~~increase in~~  
88 chlorophyll *a* concentrations and primary production (Guieu et al., 2014a). ~~This so-called~~  
89 ~~fertilizing effect has been experimentally shown using both micro- and mesocosms where the~~  
90 ~~wet deposition of Saharan dust analog strongly stimulated primary production and phytoplankton~~  
91 ~~biomass (Guieu et al., 2014a; Ridame et al., 2014) while also modifying phytoplankton diversity~~  
92 ~~(Giovagnetti et al., 2013; Lekunberri et al., 2010; Romero et al., 2011).~~ In addition, ~~besides~~  
93 ~~phytoplankton,~~ dust deposition also modified ~~also the~~ bacterial ~~community~~ assemblage ~~and led to~~  
94 ~~even~~ stronger enhancements of production and ~~or~~ respiration rates (Pulido-Villena et al., 2014).  
95 The carbon budget established from four artificial seeding experiments during the DUNE project  
96 (Guieu et al., 2014a) showed that by stimulating predominantly heterotrophic bacteria,  
97 atmospheric dust deposition can ~~enhance the heterotrophic biological behavior of these~~  
98 ~~oligotrophic waters. This has the potential to reduce the fraction of organic carbon that can be~~  
99 ~~exported~~ to deep waters during the winter mixing period (Pulido-Villena et al., 2008) and  
100 ultimately limit net atmospheric CO<sub>2</sub> drawdown.

101 ~~Another effect induced by Saharan dust deposition is the export of particulate organic~~  
102 ~~carbon (POC), as lithogenic particles can aggregate and ballast dissolved organic matter~~ (Bressac  
103 et al., 2014; Desboeufs et al., 2014; Louis et al., 2017a; Ternon et al., 2010). ~~This so-called~~  
104 lithogenic ~~carbon pump~~ can represent a major part of the carbon export following a dust  
105 deposition event (up to 50% during the DUNE experiment; Bressac et al., 2014). Recently, Louis  
106 et al. (2017a) showed that Saharan dust deposition triggers the abiotic formation of transparent  
107 exopolymeric particles (TEP), leading to the formation of organic-mineral aggregates, a  
108 formation process that is highly dependent on the quality and quantity of TEP-precursors initially  
109 present in seawater.

110 In response to ocean warming and increased stratification, nutrient cycling in the open  
111 ocean ~~is being and~~ will continue to be perturbed in the next decades ~~resulting very likely in~~  
112 regionally variable impacts (IPCC, 2019). Overall, LNLC areas are expected to expand in the  
113 future (Irwin and Oliver, 2009; Polovina et al., 2008) due to ~~a~~ thermal stratification related  
114 reduction of nutrients supply from sub-surface waters (Behrenfeld et al., 2006). As such, the role  
115 of atmospheric deposition ~~might increase as an alternative~~ source of new nutrients to surface  
116 waters. Ongoing warming and acidification ~~of the global ocean~~ (IPCC, 2019) are also evidenced  
117 in the Mediterranean Sea (e.g. Kapsenberg et al., 2017; The Mermex group, 2011). Whether or  
118 not plankton communities will respond differently to dust deposition in future conditions is still  
119 largely unknown. ~~Although dependent on resource availability,~~ it is well known that  
120 remineralisation by bacteria is subject to positive temperature control (López-Urrutia and Morán,  
121 2007). ~~As under severe nutrient limitation,~~ warming has no effect on primary productivity  
122 (Marañón et al., 2018), it will most likely further push the balance **towards net heterotrophy in**  
123 **oligotrophic areas.**

124 ~~With respect to ocean acidification,~~ an *in situ* mesocosm experiment conducted during  
125 the summer stratified period in the Northwestern Mediterranean Sea showed that the plankton

126 community was ~~rather insensitive to this perturbation~~ under strong nutrient limitation  
127 (Maugendre et al., 2017, and references therein). ~~This is coherent with results from Maugendre et~~  
~~128 al. (2015), based on a batch experiment, showing that,~~ under nutrient-depleted conditions in late  
129 winter, ocean acidification has a very limited impact on the plankton community and that small  
130 species (e.g. Cyanobacteria) might benefit from warming with a potential decrease of the export  
131 and energy transfer to higher trophic levels. In contrast, in more eutrophic coastal conditions,  
132 Sala et al. (2016) showed that ocean acidification ~~exerted~~ a positive effect on phytoplankton,  
133 especially on pico- and nano-phytoplankton. Similarly, Neale et al. (2014) showed ~~in a coastal~~  
~~134 ecosystem of the Alboran Sea~~ that ocean acidification could lead, ~~although moderately,~~ to high  
135 chlorophyll levels under low light conditions with an opposite effect under high irradiance.

136 To date and to the best of our knowledge, there have been no attempts to evaluate the  
137 behavior of plankton communities ~~after the deposition of atmospheric particles~~ in the context of  
138 future levels of temperature and pH. ~~Yet, following the recommendation from Maugendre et al.~~  
~~139 (2017), any perturbation experiment for future climate conditions in the Mediterranean Sea~~  
~~140 should consider atmospheric deposition as a source of new nutrients and consider both~~  
~~141 temperature and pH as external forcings.~~ Such experiments were conducted in the ~~frame~~ of the  
142 PEACETIME project (ProcEss studies at the Air-sEa Interface after dust deposition in the  
143 MEDiterranean sea; <http://peacetime-project.org/>) ~~during the cruise~~ on board the R/V “Pourquoi  
144 Pas?” in May/June 2017. The project aimed at ~~extensively~~ studying and parameterizing the chain  
145 of processes occurring in the Mediterranean Sea ~~after~~ atmospheric deposition ~~and to put them~~ in  
146 ~~perspective of~~ on-going environmental changes (Guieu et al., 2020). During ~~that~~ cruise, three  
147 perturbation experiments were conducted in climate reactors (300 L tanks) filled with surface  
148 water collected in the Tyrrhenian Sea (TYR), Ionian Sea (ION) and ~~in the~~ Algerian basin (FAST;  
149 Fig. 1). Six tanks were used to follow simultaneously and with a high temporal resolution, the  
150 evolution of biological activity and stocks, nutrients ~~stocks~~, dissolved organic matter as well as

151 particles dynamics and export, following a dust deposition event simulated ~~at their surface~~, both  
152 under present environmental conditions and ~~following~~ a realistic climate change scenario for  
153 2100 (ca. +3 °C and -0.3 pH units; IPCC, 2013). In this manuscript, we will present the general  
154 setup of the experiments and the evolution of nutrient and ~~biological stocks~~ (heterotrophic and  
155 autotrophic prokaryotes, photosynthetic eukaryotes as well as micro- and meso-zooplankton).  
156 ~~Several~~ other manuscripts, related to these experiments ~~and currently submitted to or published~~  
157 in this special issue, focus on plankton metabolism (primary production, heterotrophic  
158 prokaryote production) and carbon export (Gazeau et al., 2021), ~~on the~~ microbial food web  
159 (Dinasquet et al., 2021), ~~on~~ nitrogen fixation (Céline Ridame, unpublished results) and on the  
160 release of insoluble elements (Fe, Al, REE, Th, Pa) from dust (Roy-Barman et al., 2020).



## 161 2. Material and Methods

### 162 2.1. General setup

163 Six experimental tanks (300 L; Fig. 2), in which the irradiance spectrum and intensity can  
164 be finely controlled and ~~in which~~ future ocean acidification and warming conditions can be fully  
165 reproduced, were installed in a temperature-controlled container. The tanks are made of high-  
166 density polyethylene (HDPE) ~~and are trace-metal free in order to avoid contaminations,~~ with a  
167 height of 1.09 m, a diameter of 0.68 m, a surface area of 0.36 m<sup>2</sup> and a volume of 0.28 m<sup>3</sup>. ~~All~~  
~~168 tanks were cleaned before the experimental work following the protocol described by Bressac~~  
~~169 and Guieu (2013). A weak turbulence was generated by a rotating PVC blade (9 rpm) in order to~~  
~~170 mimic natural conditions.~~ Each tank was equipped with a lid containing six rows of LEDs  
171 (Alpheus©). Each of these rows were composed of blue, green, cyan and white units in order to  
172 mimic the natural sun spectrum. At the conical base of each tank, a polyethylene (PE) bottle  
173 ~~collecting the exported material from above~~ was screwed onto a polyvinyl chloride (PVC) valve  
174 that remained open during the duration of the whole experiment. Photosynthetically active  
175 radiation (PAR; 400-700 nm) and temperature were continuously monitored in each tank using  
176 respectively QSL-2100 Scalar PAR Irradiance Sensors (Biospherical Instruments©) and pt1000  
177 temperature sensors (Metrohm©) connected to a D230 datalogger (Consort©).

178 ~~The experimental protocol~~ comprised two unmodified control tanks (C1 and C2), two  
179 tanks enriched with Saharan dust (D1 and D2) and two tanks enriched with Saharan dust and  
180 maintained under warmer (+3 °C) and acidified (-0.3 pH unit) conditions (G1 and G2). The  
181 atmosphere above tanks C1, C2, D1 and D2 was flushed with ambient air (ca. 400 ppm, 6 L min<sup>-1</sup>)  
182 and tanks G1 and G2 were flushed with air enriched with CO<sub>2</sub> (ca. 1000 ppm, 6 L min<sup>-1</sup>) in  
183 order to prevent CO<sub>2</sub> degassing from the acidified tanks. CO<sub>2</sub> partial pressure (*p*CO<sub>2</sub>) in both

184 ~~ambient air~~ and CO<sub>2</sub>-enriched air was monitored using two gas analysers (LI-820, LICOR©).

185 The CO<sub>2</sub> concentration in the CO<sub>2</sub>-enriched air was manually controlled through small injections

186 of pure CO<sub>2</sub> (Air Liquide©) using a mass flow controller.

187 ~~Three experiments were performed at the long duration stations TYR, ION and FAST.~~

188 The tanks were filled by means of a ~~large~~ peristaltic pump (Verder© VF40 with EPDM hose,

189 flow of 1200 L h<sup>-1</sup>) collecting seawater below the base of the boat (depth of ~~5~~ m), used to

190 supply continuously surface seawater to a series of instruments during the entire campaign. In

191 order to homogeneously fill the tanks, the flow was divided into six HDPE pipes distributing the

192 water simultaneously into the different tanks. ~~Overall, the filling of the six tanks took 2 h~~

193 ~~(including rinsing and initial sampling, see thereafter). At the three stations, tanks were always~~

194 ~~filled at the end of the day before the start of the experiments: TYR (17/05/2017), ION~~

195 ~~(25/05/2017) and FAST (02/06/2017).~~ While filling the tanks, ~~this surface seawater was sampled~~

196 for the measurements of selected parameters (sampling time = t-12h before dust seeding, ~~see~~

197 Table 1). After filling the tanks, seawater ~~was slowly warmed~~ using 500 W heaters, controlled by

198 temperature-regulation units (COREMA©), ~~in G1 and G2 overnight~~ to reach an offset of +3 °C.

199 <sup>13</sup>C-bicarbonate was added to all tanks at 4:00 am (local time; Gazeau et al., 2021) and ~~G1 and~~

200 G2 were acidified by addition of CO<sub>2</sub>-saturated filtered (0.2 µm) seawater (~1.5 L in 300 L;

201 collected when filling the tanks at each station) ~~at 4:30 am~~ to reach a pH offset of -0.3. ~~Sampling~~

202 for ~~most~~ parameters ~~took place prior to dust seeding~~ (sampling time = t<sub>0</sub>, ~~see~~ Table 1). Dust

203 seeding was ~~performed right after t<sub>0</sub>~~ between 7:00 and 9:00 (local time) in tanks D1, D2, G1 and

204 G2. The same dust analog ~~was used and the same dust flux was simulated~~ as for the DUNE 2009

205 experiments described in Desboeufs et al. (2014). ~~Briefly, the fine fraction (< 20 µm) of Saharan~~

206 ~~soils collected in southern Tunisia, which is a major source of dust deposition over the~~

207 ~~northwestern Mediterranean basin, was used in the seeding experiments. The particle size~~

208 ~~distribution showed that 99% of particles had a size smaller than 0.1 µm, and that particles were~~

209 mostly made of quartz (40%), calcite (30%) and clay (25%; Desboeufs et al., 2014). This  
210 collected dust underwent an artificial chemical aging process by addition of nitric and sulfuric  
211 acid (HNO<sub>3</sub> and H<sub>2</sub>SO<sub>4</sub>, respectively) to mimic cloud processes during atmospheric transport of  
212 aerosol with anthropogenic acid gases (Guieu et al., 2010a, and references therein). To mimic a  
213 realistic wet flux event of 10 g m<sup>-2</sup>, 3.6 g of this analog dust were quickly diluted into 2 L of  
214 ultrahigh-purity water (UHP water; 18.2 MΩ cm<sup>-1</sup> resistivity), and sprayed at the surface of the  
215 tanks using an all-plastic garden sprayer (duration = 30 min). The N and P total contents in the  
216 dust were 1.36 ± 0.09% of N and 0.055 ± 0.003% of P (see Desboeufs et al., 2014, for a full  
217 description of dust chemical composition). The experimental protocol included the analysis of an  
218 extensive number of biogeochemical parameters and processes, not all shown and discussed in  
219 this paper, and are listed in Table 1. The experiment at stations TYR and ION lasted 72 h (3  
220 days) whereas the last experiment at station FAST was extended to four days. This relatively  
221 short duration of the experiments was constrained by the time available between stations and the  
222 time needed to properly clean the tanks between the experiments, following the protocol  
223 described by Bressae and Guieu (2013). As a larger time window was possible at the end of the  
224 cruise, the experiment at FAST was extended to four days. Seawater sampling was conducted 1  
225 h (t1h), 6 h (t6h), 12 h (t12h), 24 h (t24h), 48 h (t48h) and 72 h (t72h) (+96 h = t96h for station  
226 FAST) after dust addition. Acid-washed silicone tubes were used for transferring the water  
227 collected from the tanks to the different vials or containers. For some parameters (e.g. micro- and  
228 macro-nutrients), sampled seawater was directly filtered at the exit of the sampling tubes  
229 connected to each tank on sterile membrane filter capsules (gravity filtration with Sartobran®  
230 300; 0.2 μm).

## 231 2.2. Analytical methods

### 232 2.2.1. Carbonate chemistry

233 Seawater samples for pH measurements were stored in 300 mL glass bottles with a glass  
234 stopper, pending analysis on board (within 2 h). Samples were transferred to 30 mL quartz cells  
235 and absorbances at 434, 578 and 730 nm were measured at 25 °C on an Cary60 UV-  
236 Spectrophotometer (Agilent©) before and after addition of 50 µL of purified meta-cresol purple  
237 provided by Robert H. Byrne (University of South Florida, USA) following the method  
238 described by Dickson et al. (2007). pH on the total scale ( $pH_T$ ) was computed using the formula  
239 and constants of Liu et al. (2011). The accuracy of pH measurements was estimated to ~~0.007 pH~~  
240 ~~units~~, using a TRIS buffer solution (salinity 35, provided by Andrew Dickson, Scripps  
241 university, USA).

242 Seawater samples for total alkalinity ( $A_T$ ; ~~500 mL~~) measurements were filtered on GF/F  
243 membranes and analyzed onboard within one day.  $A_T$  was determined potentiometrically using a  
244 Metrohm© titrator (Titrando 888) and a glass electrode (Metrohm©, ecotrode plus) calibrated  
245 using first NBS buffers (pH 4.0 and pH 7.0, to check that the slope was Nernstian) and then  
246 using a TRIS buffer solution (salinity 35, provided by Andrew Dickson, Scripps university,  
247 USA). Triplicate titrations were performed on 50 mL sub-samples at 25 °C and  $A_T$  was calculated  
248 as described by Dickson et al. (2007). Titrations of standard seawater provided by Andrew  
249 Dickson (Scripps university, USA; batch 151) yielded  $A_T$  values within 5 µmol kg<sup>-1</sup> of the  
250 nominal value (standard deviation = 1.5 µmol kg<sup>-1</sup>; n = 40).

251 All parameters of the carbonate chemistry were determined from  $pH_T$ ,  $A_T$ , temperature,  
252 salinity, as well as phosphate and silicate concentrations using the R package seacarb.  
253 Propagation of errors on computed parameters was performed using the new function “error” of

254 this package, ~~considering~~ errors associated with the estimation of  $A_T$ ,  $pH_T$  as well as errors on  
255 dissociation constants (Orr et al., 2018).

## 256 2.2.2. Nutrients

257 Seawater samples for dissolved nutrients were ~~filtered directly at the exit of the sampling~~  
258 tubes ~~connected to~~ each tank (Sartobran© 300; 0.2  $\mu\text{m}$ ), ~~collected in polyethylene bottles~~ and  
259 ~~immediately~~ analyzed on board. Nitrate + nitrite ( $\text{NO}_x$ ) and silicate ( $\text{Si}(\text{OH})_4$ ) measurements  
260 were conducted using a segmented flow analyzer (AAIII HR Seal Analytical©) according to  
261 Aminot and K  rouel (2007) with a ~~limit of quantification~~ of 0.05  $\mu\text{mol L}^{-1}$  for  $\text{NO}_x$  and 0.08  
262  $\mu\text{mol L}^{-1}$  for  $\text{Si}(\text{OH})_4$ . In addition, ~~for t-12h samples, the analysis of  $\text{NO}_x$  was also performed by~~  
263 ~~a spectrometric method in the visible~~ at 540 nm, with a 1 m Liquid Waveguide Capillary Cell  
264 (LWCC). ~~The limit of detection was~~  $\sim 10 \text{ nmol L}^{-1}$  ~~and the reproducibility was~~  $\sim 6\%$ . ~~Also from~~  
265 ~~samples taken at t-12h, the measurement of ammonium concentrations was performed~~ on board  
266 using a Fluorimeter TD-700 (Turner Designs©) according to Holmes et al. (1999). This  
267 ~~fluorimetric~~ method is based on the reaction of ammonia with orthophthaldialdehyde and sulfite  
268 and has a ~~limit of quantification~~ of 0.01  $\mu\text{mol L}^{-1}$ . Dissolved inorganic phosphorus (DIP)  
269 concentrations were quantified using the Liquid Waveguide Capillary Cell (LWCC) method  
270 according to Pulido-Villena et al. (2010). The LWCC was 2.5 m long and the ~~limit of detection~~  
271 was 1  $\text{nmol L}^{-1}$ .

## 272 2.2.3. Pigments

273 ~~A volume of 2.5 L of sampled seawater was~~ filtered onto GF/F filters, immediately  
274 frozen in liquid nitrogen and stored at  $-80 \text{ }^\circ\text{C}$  pending analysis at the SAPIGH analytical platform  
275 at the Institut de la Mer de Villefranche (IMEV, France). Filters were ~~extracted~~ at  $-20 \text{ }^\circ\text{C}$  in 3 mL  
276 methanol (100%) containing an internal standard (vitamin E acetate, Sigma©), ~~disrupted by~~

277 ~~sonication~~ and clarified one hour later by vacuum filtration through GF/F filters. The extracts  
278 were rapidly analyzed (within 24 h) on a complete Agilent© Technologies 1200 series HPLC  
279 system. The pigments were separated and quantified as described in Ras et al. (2008).

## 280 **2.2.4. Flow cytometry**

281 For ~~the enumeration of autotrophic prokaryotic and eukaryotic cells, heterotrophic~~  
~~282 prokaryotes and heterotrophic nanoflagellates (HNF) by~~ flow cytometry, subsamples (4.5 mL)  
283 were fixed with glutaraldehyde grade I ~~25%~~ (1% final concentration), and incubated for 30 min  
284 at 4 °C, ~~then~~ quick-frozen in liquid nitrogen and stored at -80 °C until analysis. Samples were  
285 thawed at room temperature. Counts were performed on a FACSCanto II flow cytometer (Becton  
286 Dickinson©) equipped with 3 air-cooled lasers: blue (argon 488 nm), red (633 nm) and violet  
287 (407 nm). ~~The separation of different autotrophic populations was based on their scattering and~~  
~~288 fluorescence signals according to~~ Marie et al. (2010). *Synechococcus* spp. was discriminated by  
289 its strong orange fluorescence ( $585 \pm 21$  nm), and pico- and nano-eukaryotes were discriminated  
290 by their scatter signals of red fluorescence ( $> 670$  nm). For the enumeration of heterotrophic  
291 prokaryotes, cells were stained with SYBR Green I (Invitrogen – Molecular Probes) at 0.025%  
292 (vol / vol) final concentration for 15 min at room temperature in the dark. Stained prokaryotic  
293 cells were discriminated and enumerated according to their right-angle light scatter (SSC) and  
294 green fluorescence at 530/30 nm. ~~In a plot of green versus red fluorescence, heterotrophic~~  
295 prokaryotes were distinguished from autotrophic prokaryotes. For the enumeration of HNF,  
296 ~~staining was performed with SYBR Green I (Invitrogen – Molecular Probes) at 0.05% (v/v) final~~  
297 ~~concentration for 15-30 min at room temperature in the dark (Christaki et al., 2011). Cells were~~  
~~298 discriminated and enumerated according to their SSC and green fluorescence at 530/30 nm.~~  
299 Fluorescent beads (1.002  $\mu\text{m}$ ; Polysciences Europe©) were ~~systematically~~ added to ~~each~~  
300 ~~analyzed~~ sample as internal standard. ~~The cell abundance was determined from the~~ flow rate,

301 ~~which was calculated~~ with TruCount beads (BD biosciences©). Biomasses of each group were  
302 estimated based on conversion equations and/or factors found in the literature (see section 2.3.2).

## 303 **2.2.5. Micro-phytoplankton and -heterotrophs**

304 At t-12h (~~i.e. seawater sampled during the filling of the tanks~~), a volume of 500 mL ~~was~~  
305 ~~sampled~~ in glass vials and immediately preserved in a 5% acidic Lugol's solution ~~pending~~  
306 ~~analysis~~. At the Laboratoire d'Océanographie de Villefranche (LOV, France), 100 mL aliquots  
307 were transferred to sedimentation chambers (Utermohl) and counted under an inverted  
308 microscope at 200 to 400 magnifications.

## 309 **2.2.6. Meso zooplankton**

310 At the end of each experiment (~~t+72h for TYR and ION and t+96 h for FAST, after~~  
311 ~~artificial dust seeding~~), the ~~sediment traps~~ were removed, ~~closed and stored~~ with formaldehyde  
312 4% (see Gazeau et al., 2021). ~~The~~ valve at the base of ~~the~~ tanks ~~was then re-opened to let the~~  
313 remaining water inside the tanks (~~TYR=165-180 L; ION= 172.5 L and FAST= 150 L~~) pass  
314 through a ~~large~~ PVC sieve (~~100 µm~~). The organisms retained ~~on that mesh~~ were gently removed  
315 ~~from the sieve~~ using a washing bottle filled with filtered seawater (0.2 µm), and transferred  
316 directly inside a 250 mL bottle. ~~The bottle was filled with the sample (1/3 of the volume), and~~  
317 ~~was completed with formaldehyde 4%. The zooplankton digital images were obtained~~ using a  
318 ZooSCAN (Hydroptic©; Gorsky et al., 2010) at the PIQv-platform of EMBRC-France. ~~The~~  
319 ~~identification of species was performed by~~ automatic classification with a reference dataset in  
320 EcoTaxa (<https://ecotaxa.obs-vlfr.fr/>, last access: 17/04/2020) and ~~then all~~ validated and  
321 ~~corrected manually~~.

## 322 **2.3. Data analyses**

### 323 **2.3.1. Nutrient inputs from dust**

324 The maximum percentage of dust-born dissolved N and P was ~~calculated considering that~~  
325 ~~these evapo-condensated dust contain  $1.36 \pm 0.09\%$  of N and  $0.055 \pm 0.003\%$  of P (Desboeufs et~~  
326 ~~al., 2014). Based on maximal concentrations observed in the D and G tanks after seeding (two~~  
327 ~~discrete sampling within 6 h following dust seeding,  $t_{1h}$  and  $t_{6h}$ ), one can estimate the maximal~~  
328 ~~% of dissolution of dust in seawater during the three experiments;~~

$$329 \quad \%_{dissolution} = \frac{CONC_{max} - CONC_{init}}{CONC_{dust}} \cdot 100 \quad (1)$$

330 where  $CONC_{init}$  is the concentration of the corresponding nutrient in each tank before seeding  
331 ( $t_0$ ),  $CONC_{max}$  corresponds to the concentration of the corresponding nutrient in each tank when  
332 nutrient concentration was at a maximum ~~over~~ the first 6 h after seeding ~~as observed based on~~  
333 ~~our discrete sampling procedure~~, and  $CONC_{dust}$  is the maximum ~~addition, corresponding to a~~  
334 100% dissolution ~~of its total concentration in the~~ dust analog (~~as estimated~~ based on dust  
335 ~~chemical composition~~; Desboeufs et al., 2014; ~~see above~~).

### 336 **2.3.2. Autotrophic and heterotrophic biomass**

337 ~~As~~ micro-phytoplankton ~~counting was not performed throughout the~~ experiment, as a  
338 first approximation, autotrophic biomass was ~~calculated~~ as the sum of ~~carbon contained in~~  
339 *Synechococcus*, ~~pico-eukaryotes~~ and nano-eukaryotes (~~abundances based on flow cytometry~~) ~~and~~  
340 ~~is therefore restricted to the fraction  $< 20 \mu\text{m}$ . For *Synechococcus*, conversion to carbon units~~  
341 ~~was done considering  $250 \text{ fg C cell}^{-1}$  (Kana and Glibert, 1987), while the equation proposed by~~  
342 ~~Verity et al. (1992;  $0.433 \text{ BV}^{0.863}$  where BV refers to the biovolume)~~ was used for pico- and  
343 nano-eukaryotes assuming a spherical shape and a diameter of 2 and 6  $\mu\text{m}$  ~~for the two groups~~,



344 respectively. Percentages of these different groups were calculated in order to estimate the  
345 composition of the communities at the start and its evolution during the experiments.  
346 Furthermore, heterotrophic biomass was computed as the sum of heterotrophic prokaryotes  
347 biomass and heterotrophic nanoflagellates biomass. For heterotrophic prokaryotes, conversion to  
348 carbon units were done considering 20 fg C cell<sup>-1</sup> (Lee and Fuhrman, 1987) and for heterotrophic  
349 nanoflagellates assuming 220 fg C μm<sup>-3</sup> (Børsheim and Bratbak, 1987), a spherical shape and a  
350 diameter of 3 μm. The ratio of autotrophic and heterotrophic biomass during the experiments was  
351 used to evaluate the trophic status of the investigated communities and its evolution. Finally, a  
352 proxy for micro-phytoplankton biomass ( $B_{\text{micro}}$ ) was estimated following Vidussi et al. (2001), as  
353 the sum of Fucoxanthin and Peridinin.

## 354 3. Results

### 355 3.1. Initial conditions

356 Initial conditions of ~~various measured parameters~~ at the three sampling stations while  
357 filling the tanks (t-12h before seeding) are shown in Table 2. pH<sub>T</sub> and total alkalinity  
358 concentrations ~~followed a west to east increasing gradient (8.03, 8.04 and 8.07; 2443, 2529 and~~  
359 ~~2627  $\mu\text{mol kg}^{-1}$  at FAST, TYR and ION, respectively).~~ NO<sub>x</sub> concentrations were maximal at  
360 station FAST with a NO<sub>x</sub>:DIP molar ratio of 4.6. Very low NO<sub>x</sub> concentrations were observed  
361 at stations TYR and ION (14 and 18  $\text{nmol L}^{-1}$ , respectively). DIP concentrations were the highest  
362 at station TYR (17  $\text{nmol L}^{-1}$ ) and the lowest at the most eastern station (ION, 7  $\text{nmol L}^{-1}$ ).  
363 Consequently, the lowest NO<sub>x</sub>:DIP ratio was measured at TYR (0.8), compared to ION and  
364 FAST (2.8 and 4.6, respectively). Ammonium concentrations were maximal at TYR (0.045  $\mu\text{mol}$   
365  $\text{L}^{-1}$ ), intermediate at ION (0.022  $\mu\text{mol L}^{-1}$ ), and minimal at FAST (below detection limit).  
366 Silicate concentrations were similar at stations TYR and ION ( $\sim 1 \mu\text{mol L}^{-1}$ ) and higher than at  
367 station FAST (0.64  $\mu\text{mol L}^{-1}$ ).

368 Very low and similar concentrations of chlorophyll *a* were measured at the three stations  
369 (0.063 - 0.072  $\mu\text{g L}^{-1}$ ). The proportion of the different major pigments (Fig. 3) showed that  
370 phytoplankton communities at stations TYR and ION were very similar with a dominance of  
371 Prymnesiophytes (i.e. 19'-hexanoyloxyfucoxanthin; Ras et al., 2008) followed by Cyanobacteria  
372 (i.e. Zeaxanthin; Ras et al., 2008). In contrast, at station FAST, the plankton community was  
373 clearly dominated by photosynthetic prokaryotes (i.e. Zeaxanthin and Divinyl-chlorophyll *a*;  
374 Cyanobacteria and Prochlorophytes, respectively; Ras et al., 2008). At all three stations, the  
375 proportion of pigments representative of larger species (i.e. Fucoxanthin and Peridinin; diatoms  
376 and dinoflagellates respectively; Ras et al., 2008) were very small (< 5% for each pigment).

377 Cellular abundances of all studied microorganisms (phytoplankton, micro-grazers,  
378 heterotrophic bacteria) were the highest at FAST (Table 2). Picocukaryotes, *Synechococcus* and  
379 heterotrophic prokaryotes abundances followed an east to west increasing trend (ION < TYR <  
380 FAST). In contrast, nano-cukaryotes abundance was similar at FAST and ION, and minimal at  
381 TYR. The abundance of heterotrophic nanoflagellates (HNF) were similar at TYR and FAST  
382 (~110-125 cells mL<sup>-1</sup>), twice as high as the one observed at station ION. This east to west  
383 increasing trend was also observed for micro-phytoplankton and micro-heterotrophs abundances  
384 (microscopic analyses; Table 2). The ratio between autotrophic biomass and heterotrophic  
385 biomass was clearly in favor of the heterotrophic compartment at stations TYR and FAST (~0.6  
386 at the two stations) but the opposite was found at station ION (ca. 1.3).

## 387 3.2. Conditions of irradiance, temperature and pH during 388 the experiments

389 Irradiance levels, during the experiments in the control tanks (C1, C2), were maximal at  
390 station ION and minimal at station FAST (daily average maximum levels in controls: ~1050,  
391 1130 and ~1020  $\mu\text{mol photons m}^{-2} \text{s}^{-1}$  at TYR, ION and FAST, respectively; Fig. 4). Decreases  
392 of water transparency after dust addition was observed at all three stations with a maximum dust  
393 impact at station ION and the lowest impact at station FAST where irradiance levels decreased  
394 by only 60  $\mu\text{mol photons m}^{-2} \text{s}^{-1}$  after dust addition (average between tanks D and G). At station  
395 TYR, a more pronounced decrease was observed in acidified and warmed tanks (G1 and G2)  
396 with a decrease of daily average maximum irradiance of ~60 and ~160  $\mu\text{mol photons m}^{-2} \text{s}^{-1}$  as  
397 compared to dust-amended tanks D and controls, respectively. Temperature control (Fig. 4) was  
398 not optimal showing deviations between replicates of treatment G of up to 1.5 °C (station ION).  
399 Temperature in controls and D tanks displayed a daily cycle with an increase during the day and

400 a decrease at night. Overall, the differences between the warmed treatment (G) and the other  
401 tanks were +3, +3.2 and +3.6 °C at TYR, ION and FAST, respectively.

402 Addition of CO<sub>2</sub>-saturated filtered seawater led to a decrease of pH<sub>T</sub> from 8.05 ± 0.004  
403 (average ± SD between C1, C2, D1 and D2 at t0) to 7.74 (average between G1 and G2) at station  
404 TYR, from 8.07 ± 0.002 to 7.78 at station ION and 8.05 ± 0.001 to 7.72 at station FAST (Fig. 5).  
405 pH<sub>T</sub> levels remained more or less constant in ambient pH levels tanks during all three  
406 experiments with no clear impact of dust addition in tanks D1 and D2. In lowered pH tanks, pH  
407 levels gradually increased during the experiments with a systematic larger increase in one of the  
408 duplicates (G1). Yet pH<sub>T</sub> increases remained moderate thanks to the flushing of CO<sub>2</sub>-enriched air  
409 above the tanks (*p*CO<sub>2</sub> of 1017 ± 11, 983 ± 96, 1023 ± 25 ppm at TYR, ION and FAST,  
410 respectively; data not shown). Partial pressure of CO<sub>2</sub> in ambient air was similar at the three  
411 stations, i.e. 410 ppm (data not shown). At all three stations, the addition of <sup>13</sup>C-bicarbonate to  
412 all tanks before t0 led to an increase of total alkalinity between 6 and 11 μmol kg<sup>-1</sup> at t0. Dust  
413 addition, performed right after t0 in tanks D and G, led to a *A*<sub>T</sub> decrease in these tanks between 8  
414 and 16 μmol kg<sup>-1</sup> at t24h with no apparent effects of warming and acidification. Overall, no large  
415 changes in this parameter were observed during the experiments (Fig. 5).

### 416 3.3. Changes in nutrient concentrations

417 Dust addition in tanks D and G led to a rapid and maximum input of NO<sub>x</sub> (as observed  
418 during the first 6 h; Fig. 6; Table 3) of 11 μmol L<sup>-1</sup> at all three stations with no differences  
419 between both treatments. The corresponding dissolution percentage of N contained in the dust  
420 analog was between 94 and 99%. In contrast, maximum DIP release (within 6 h after dust  
421 addition) from the dust analog was much smaller and comprised between 20 and 37 nmol L<sup>-1</sup>,  
422 with slightly higher release at FAST (31-37 nmol L<sup>-1</sup>) as compared to the other stations.  
423 Dissolution percentages for DIP were estimated between 9.2 and 17.3% of total phosphorus

424 contained in dust. As a consequence ~~of these contrasted dissolution of N and P~~,  $\text{NO}_x$ :DIP ratios  
425 increased from initial values below 5 to above 300, within 6 h after dust seeding, in ~~the dust~~  
426 ~~amended (D and G) tanks~~ (Fig. 6).

427 After these rapid increases ~~due to N and P releases in dust amended tanks~~, both variables  
428 decreased with time. While nutrient variability was small in control tanks ~~over the duration of the~~  
429 ~~experiments~~ ( $\text{NO}_x$  and DIP variations below 20 and 3  $\text{nmol L}^{-1}$ , respectively), large decrease of  
430 both elements ~~was measured~~ in dust amended tanks (D and G; Table 4). For  $\text{NO}_x$ , similar linear  
431 decreases were observed throughout the experiments at stations TYR and ION with no visible  
432 differences between tanks D and G. In contrast, at station FAST, a more pronounced decrease in  
433  $\text{NO}_x$  was observed in dust-amended (D and G) tanks ~~as compared to the other stations, with~~  
434 ~~detectable larger decreases~~ in warmed and acidified tanks relative to the D treatment.

435 Nevertheless, at all stations,  $\text{NO}_x$  concentrations in D and G treatments remained far above  
436 ambient levels throughout the experiments ( $> 9 \mu\text{mol L}^{-1}$ ). Abrupt decreases in DIP were  
437 observed during the three experiments after the initial increase. At station TYR, after 24 h, all  
438 DIP released from dust decreased to initial levels in tanks G while it took two more days to reach  
439 initial levels in tanks D. In contrast, at station ION, no clear difference in DIP dynamics was  
440 observed between treatments D and G, with concentrations that decreased rapidly during the first  
441 24 h but ~~that~~ remained above initial levels until the end of the experiment. At station FAST,  
442 similarly to station TYR, DIP decreased rapidly from t12h in treatment G, reaching levels close  
443 to initial conditions at the end of the experiment. DIP decrease was much lower in treatment D  
444 (Table 4) with concentrations maintained far above ambient levels throughout the experiment.  
445 As a consequence of these differences between  $\text{NO}_x$  and DIP dynamics as well as differences  
446 among stations,  $\text{NO}_x$ :DIP ratio increased ~~during the experiments~~ with clear differences between  
447 stations (Fig. 6) and remained much higher than ~~that~~ in the controls ~~over the duration of the three~~  
448 ~~experiments~~.

449 Silicate dynamics showed at all stations higher concentrations in dust amended (D and G)  
450 tanks relative to the controls. At TYR, while concentrations remained stable in control tanks,  
451 they increased linearly with time in the other tanks (D and G) with no apparent effect of the  
452 imposed increase in temperature and decrease in pH (i.e. tanks G). Difference of  $\text{Si(OH)}_4$   
453 concentration between dust amended treatments (D and G) and controls was  $\sim 0.1 \mu\text{mol L}^{-1}$  at the  
454 end of the experiment. At station ION, after an initial decrease of concentrations between t-12h  
455 and t0, concentrations increased in all tanks until the end of the experiment with higher  
456 concentration in dust amended tanks (D and G) than in controls (no difference between D and G  
457 treatments). In contrast, at FAST, concentrations increased between t-12h and t0, and continued  
458 to increase in all tanks (with higher values in dust amended tanks) until t48h and then decreased  
459 until the end of the experiment. At the end of the experiment (t96h),  $\text{Si(OH)}_4$  concentration was  
460 higher in the G treatment than in the D treatment which was similar to the controls.

### 461 3.4. Changes in biological stocks

462 ~~Regarding biological stocks,~~ temporal dynamics showed very different patterns amongst  
463 ~~the three studied~~ stations. At TYR, total chlorophyll *a* concentrations did not change in dust  
464 amended tanks ~~maintained under ambient levels of temperature and pH~~ (Fig. 7) and even led to  
465 slightly decreased values 24 h after dust addition (e.g. -35 to -38% in D1 and D2, respectively as  
466 compared to controls; Table 5). No clear effect of dust addition (tanks D vs. C) were detectable  
467 for all groups based on pigment analyses (Fig. 7). Results obtained based on flow cytometry  
468 counting (Fig. 8) were coherent with these observations and showed stronger decreases in cell  
469 abundances for  $< 20 \mu\text{m}$  autotrophic groups in tanks D1 and D2 (-77 to -80%). In contrast, ~~at this~~  
470 ~~station,~~ the abundance of heterotrophic prokaryotes (HP) increased rapidly after dust addition  
471 both under ambient (+53-68%) and future (+68%) environmental conditions, with no clear  
472 difference among ~~those~~ treatments. In warmed and acidified tanks, strong discrepancies between

473 the duplicates were observed for pigments and autotrophic cell abundances. ~~Indeed,~~ tank G1  
474 showed ~~moderately higher levels~~ for all variables ~~as compared to tanks C~~ with the exception of  
475 **pico-eukaryotes**, while in G2 all variables responded strongly to dust addition with maximum  
476 relative changes of > 300% (with the exception of **nano-eukaryotes**: +119%). While HNF  
477 abundances responded positively to the treatments in D1, D2 and G2 (+100-352%), abundances  
478 increased sharply in tank G1 towards the end of the experiment (+1095%).

479 At ION, a clear ~~distinction~~ between treatments ~~could be~~ observed for almost all pigments  
480 and cell abundances (Fig. 7, Fig. 8). With the exception of **nano-eukaryotes** and HNF, all  
481 variables (pigments and cell abundances) increased as a response to both dust addition and  
482 warmed/acidified conditions (i.e. ~~C < D < G~~). ~~As an example~~ (Table 5), the maximum relative  
483 changes as compared to controls observed for total chlorophyll *a* were 109-183% and 399-426%  
484 in tanks D and G, respectively. The highest stimulation to dust addition was observed for  
485 *Synechococcus* with a +317-390% ~~increase~~ and +805-1425% increase in D and G tanks  
486 respectively (Table 5). ~~Abundances of~~ nano-eukaryotes and HNF ~~suggested~~ no impact of dust  
487 addition under ambient conditions but a ~~positive impact~~ in treatment G. In contrast to ~~what was~~  
488 ~~observed~~ at TYR for ~~HP abundances~~, an effect of temperature and pH ~~was observed~~ at station  
489 ION with a higher impact of dust addition under future environmental conditions.

490 At station FAST, all ~~above mentioned variables related to~~ biological stocks increased  
491 strongly after dust addition (Fig. 7, Fig. 8 and Table 5). ~~For instance,~~ total chlorophyll *a*  
492 increased ~~following an exponential trend~~ until the end of the experiment ~~reaching maximal~~  
493 ~~values at t96h~~ with slightly lower values observed under ambient environmental conditions  
494 (+237-318% in D tanks ~~vs.~~ ~ +400% in G tanks). Prymnesiophytes (i.e. 19'-  
495 hexanoyloxyfucoxanthin) and diatoms (i.e. Fucoxanthin) appeared as the groups benefiting the  
496 most from dust addition with no large impacts of warming/acidification. ~~In contrast,~~  
497 Pelagophytes (i.e. 19'-butanoyloxyfucoxanthin) and green algae (i.e. Total Chlorophyll *b*)

498 ~~responded much more~~ in treatment G ~~than in treatment D~~. Finally, although Cyanobacteria (i.e.  
499 Zeaxanthin) responded faster to dust addition under future environmental conditions (tanks G),  
500 this effect ~~tended to attenuate~~ towards the end of the experiment. In contrast to estimates based  
501 on ~~HPLC data~~, increases in cell abundances did not generally ~~take place~~ until the end of the  
502 experiment. While abundances ~~in~~ pico-eukaryotes increased until t96h in treatment D,  
503 abundances sharply declined between t72h and t96h for this group in treatment G. The same  
504 trend was observed for *Synechococcus* ~~during this experiment~~, although discrepancies between  
505 duplicates in treatment D at ~~sampling time~~ t96h did not allow drawing conclusions on the  
506 behavior of this group ~~at~~ the end of the experiment. ~~Both under ambient and future conditions~~,  
507 abundances of ~~nano-eukaryotes~~ declined sharply between t72h and t96h. The decline in HP  
508 abundances ~~appeared even~~ earlier during the experiment with moderate maximum relative  
509 differences as compared to controls ~~observed~~ at t48h. HP abundances declined very sharply  
510 between t48h and t96h in treatment G, reaching control levels, while this decline was less sharp  
511 under ambient ~~environmental levels~~. Finally, HNF dynamics during this experiment was hard to  
512 ~~evaluate with no clear effects of dust addition or pH/temperature conditions and with a large~~  
513 increase in abundances in only one duplicate of treatment G (t24h) followed by a gradual  
514 ~~decrease~~.

515 Abundances of meso-zooplankton at the end of the experiments showed relatively similar  
516 values at stations TYR and ION while much higher levels were observed at station FAST (Fig.  
517 9). As a consequence of large variability between duplicates at stations TYR and ION, no clear  
518 effects of treatments were detected. At station FAST, although the sample size was too low to  
519 statistically test for differences, higher total abundances of meso-zooplankton species were  
520 observed in the dust-amended tanks with no differences between ambient and future conditions  
521 of temperature and pH. However, differences in abundance were visible between these two



- 522 treatments for specific groups, with respectively higher abundance of Harosa and lower
- 523 abundance of Crustacea (other than copepods) and Mollusca in warmed and acidified tanks.

## 524 4. Discussion

### 525 4.1. Initial conditions

526 ~~Over the transect, the mixed layer occupied the first 20 m. It was shallower at TYR as~~  
527 ~~compared to ION and FAST (mixed layer depth, MLD of ~ 10 vs ~15 m, respectively) at the~~  
528 ~~time of the sampling (Van Wambeke et al., 2020a). Such shallow MLD is well representative of~~  
529 ~~stratified conditions encountered in the western Mediterranean basin in late spring/early summer~~  
530 ~~(D'Ortenzio et al., 2005). Overall, the three experiments were conducted with surface seawater~~  
531 ~~collected during~~ oligotrophic conditions typical of the open Mediterranean Sea at this period of  
532 the year (late spring). Although direct measurements of NO<sub>x</sub> and DIP concentrations using  
533 nanomolar techniques (as performed in our study) are scarce in the Mediterranean Sea, the low  
534 levels measured during the cruise are in agreement with DIP values reported for the three ~~studied~~  
535 ~~basins (Djaoudi et al., 2018) and with NO<sub>x</sub> and DIP concentrations measured in coastal waters of~~  
536 ~~Corsica in late spring/early summer (Louis et al., 2017b; Pulido-Villena et al., 2014; Ridame et~~  
537 ~~al., 2014). Furthermore, at all three stations, NO<sub>x</sub>:DIP molar ratios in the tested surface waters~~  
538 ~~were well below the Redfield ratio (16:1) and are consistent with ratios found in these previously~~  
539 ~~cited studies. Both low NO<sub>x</sub>:DIP ratio and low nutrient concentrations suggest that communities~~  
540 ~~found at the three stations experienced N and P co-limitation at the start of the experiments, as~~  
541 ~~previously shown by Tanaka et al. (2011). A side nutrient enrichment experiment confirmed that,~~  
542 ~~at the three sites, heterotrophic bacteria were mainly N-P co-limited (Van Wambeke et al.,~~  
543 ~~2020b). In contrast to N and P, initial concentrations of dissolved Fe in the sampled seawater,~~  
544 ~~ranging~~ from 1.5 nmol L<sup>-1</sup> at TYR to 2.5 nmol L<sup>-1</sup> at ION (Roy-Barman et al., 2020), were  
545 unlikely limiting for biological activity as previously shown in the Mediterranean Sea under  
546 stratified conditions (Bonnet et al., 2005; Ridame et al., 2014).

547 Low total chlorophyll *a* concentrations in the tested waters were representative of surface  
548 concentrations reported for the Western and Central Mediterranean Sea in late spring/early  
549 summer, both from remote sensing images (Bosc et al., 2004), and from *in situ* measurements  
550 provided in a database from Manca et al. (2004). While large species (i.e. diatoms,  
551 dinoflagellates) represented only ~10% of the total chlorophyll *a* biomass of the tested waters,  
552 the composition of the smaller size phytoplankton communities differed substantially. Indeed,  
553 communities were clearly dominated by nano-eukaryotes at stations TYR and ION and a larger  
554 contribution from pico-eukaryotes and Cyanobacteria was observed at station FAST. Due to their  
555 low competitiveness under nutrient limitation, the small contribution of large phytoplankton cells  
556 at the start of the experiment is a fingerprint of LNLC areas in general, and of surface  
557 Mediterranean waters in late spring and summer (Siokou-Frangou et al., 2010).

558 As biomass of both heterotrophic nanoflagellates and prokaryotes followed a west to east  
559 gradient (FAST > TYR > ION), the ratio of autotrophic vs heterotrophic biomass appeared  
560 clearly in favor of the heterotrophic compartment at stations TYR and FAST (ratio of 0.6) while  
561 a value above 1 was estimated at ION (ratio of 1.3). This is coherent with the highest net  
562 community production (NCP) rates being reported at this station by Gazeau et al. (2021)  
563 showing that the initial community at the start of this experiment was very close to metabolic  
564 balance (mean  $\pm$  SE:  $-0.06 \pm 0.09 \mu\text{mol O}_2 \text{ L}^{-1} \text{ d}^{-1}$ ). The highest community respiration rates and  
565 consequently lowest NCP rates were measured at station TYR ( $-1.9 \mu\text{mol O}_2 \text{ L}^{-1} \text{ d}^{-1}$ ) further  
566 suggesting that the autotrophic plankton community was not very active and relying on  
567 regenerated nutrients, as shown by the highest level of  $\text{NH}_4^+$  measured at the start of this  
568 experiment. In contrast, although slightly heterotrophic (Gazeau et al., 2021) and limited by the  
569 low amount of nutrients, the community of the tested waters at FAST was the most active as  
570 shown by the highest levels of  $^{14}\text{C}$  production and heterotrophic prokaryote production (Gazeau  
571 et al., 2021) as well as  $\text{N}_2$  fixation (Céline Ridame, unpublished results). Altogether, the

572 heterotrophic signature of the three investigated stations, although closer to metabolic balance at  
573 ION, reflected typical biogeochemical conditions in the Mediterranean Sea during late spring to  
574 early summer (Regaudie-de-Gioux et al., 2009).

## 575 **4.2. Critical assessment of the experimental system and** 576 **methodology**

577 The experimental tanks used in this study have been successfully validated in previous  
578 studies designed to investigate the inputs of macro- and micro-nutrients (e.g. NO<sub>x</sub>, DIP, DFe)  
579 and the export of organic matter, ~~under close-to-abiotic conditions (seawater filtration onto 0.2~~  
580 ~~µm)~~ following simulated wet dust events using the same analog as used in our study (Bressac  
581 and Guieu, 2013; Louis et al., 2017a, 2018). Louis et al. (2017a, 2018) further investigated these  
582 impacts under lowered pH conditions, ~~although no control of atmospheric pCO<sub>2</sub> was performed~~  
583 resulting in a rapid increase of pH levels in the acidified filtered seawater due to CO<sub>2</sub> outgassing  
584 (from ~7.4 to ~7.7 in six days). ~~Since those above-mentioned studies, in order to avoid this, we~~  
585 ~~improved~~ our experimental system ~~to allow mimicking future conditions by controlling~~  
586 atmospheric pCO<sub>2</sub> in addition to light and temperature (i.e. climate reactors). ~~This allowed to~~  
587 significantly reduce CO<sub>2</sub> outgassing and maintain pH levels close to ~~experimental~~ targets. ~~Still,~~  
588 ~~as illustrated in Fig. 5, the~~ regulation of atmospheric CO<sub>2</sub> was consistently more efficient in tank  
589 G2 compared to G1, resulting in a small discrepancy in terms of pH (highest difference of 0.04  
590 pH units between the two G tanks at FAST), possibly due to a potential leak or a longer flushing  
591 time above tank G1. Nevertheless, as no systematic differences in ~~terms of~~ biological response  
592 were observed between these two tanks, ~~we believe that~~ these small differences in ~~terms of~~  
593 ~~regulated~~ pH had no ~~consequences~~ on the obtained results.

594 The lids above tanks, equipped with LEDs in order to reproduce sunlight intensity and  
595 spectrum, were used for the first time during these experiments. While simulated intensities were

596 close to estimates for the Northwestern Mediterranean Sea at 5 m depth in June (~1100  $\mu\text{mol}$   
597 photons  $\text{m}^{-2} \text{s}^{-1}$ ; Bernard Gentili, personal communication, 2017) and fairly consistent between  
598 duplicates under control and dust-amended conditions, larger differences were observed between  
599 ~~the two warmed and acidified tanks. The reasons of~~ these discrepancies could result from small  
600 differences ~~in terms of light intensity regulation between lids, of~~ PAR sensors calibration and/or  
601 of different turbidity related to the amount of particles remaining in the tanks. As for pH  
602 ~~discussed above,~~ replication in terms of biological response appeared satisfactory ~~for this~~  
603 ~~treatment (except at station TYR; see below), and we believe these technical issues had no~~  
604 ~~significant impacts on our results.~~

605 Continuous measurements in the tanks showed that temperature was not spatially  
606 homogeneous, leading to significant differences among replicates. This was ~~especially the case~~  
607 for warmed tanks (treatment G) ~~for which~~ a maximal average difference over the experimental  
608 period of 0.7 °C ~~was observed~~ during the FAST experiment. ~~As for the other controlled~~  
609 ~~parameters discussed above,~~ these discrepancies did not systematically lead to observable  
610 differences in the investigated stocks and processes between duplicates (except at TYR, see  
611 below).

612 The ~~relatively low number of experimental units that could be installed inside an~~  
613 ~~embarkable~~ clean container ~~restrained~~ our possibility to ~~consider more than two~~ replicates per  
614 treatment. ~~Fortunately, as already said,~~ differences between duplicates were, for the vast majority  
615 of studied variables and processes, lower than differences between treatments and appear  
616 ~~acceptable~~ considering the difficulty to incubate plankton communities for which slight  
617 differences in ~~their~~ initial composition can translate into ~~very~~ important differences in dynamics  
618 (Eggers et al., 2014). Nevertheless, ~~we have to note that~~ important discrepancies were detected  
619 ~~regarding~~ autotrophic stocks and processes (Gazeau et al., 2021) for ~~tanks of~~ the warmed and  
620 acidified treatment at station TYR. The reasons behind these differences are ~~not fully understood~~

621 ~~but we strongly suspect that~~ heterotrophic nano-flagellates, ~~feeding mainly~~ on prokaryotic  
622 picoplankton (Sherr and Sherr, 1994), ~~exerted a strong top-down control on this group~~ in tank G1  
623 ~~in which~~ HNF abundance sharply increased during the experiment. ~~All in all~~, while the  
624 methodology used in this study allowed to successfully evaluate the impacts of dust addition  
625 under both present and future environmental conditions at two out of three tested waters, these  
626 discrepancies at station TYR prevent us from drawing any strong conclusion on the effect of dust  
627 addition on the dynamics of the community under future environmental conditions at that station.

### 628 **4.3. Impact of dust addition under present environmental** 629 **conditions**

630 During ~~the three~~ experiments, the observed increases in NO<sub>x</sub> and DIP few hours after  
631 dust addition under present environmental conditions were ~~rather~~ similar to the enrichment ~~levels~~  
632 obtained during the DUNE experiments **at the surface of the mesocosms (~ 50 m<sup>3</sup>)** after the  
633 simulation of a wet dust deposition using the same dust analog and the same simulated flux  
634 (Pulido-Villena et al., 2014; Ridame et al., 2014). The intensity of ~~this~~ simulated wet deposition  
635 event (i.e. 10 g m<sup>-2</sup>) represents a high but realistic scenario, as several studies reported even  
636 higher short wet deposition events in this area of the Mediterranean Sea (Bonnet and Guieu,  
637 2006; Loÿe-Pilot and Martin, 1996; Ternon et al., 2010). Furthermore, based on previous studies  
638 reporting the mixing between dust and polluted air masses during the atmospheric transport of  
639 dust particles (e.g. Falkovich et al., 2001; Putaud et al., 2004), we ~~chose to use an~~ evapo-  
640 condensed dust analog that mimics the processes taking place in the atmosphere prior to  
641 deposition, essentially the adsorption of inorganic and organic soluble species (e.g. sulfate and  
642 nitrate; see Guieu et al., 2010a, for further details). The imposed evapo-condensation processes  
643 are responsible for the large nitrate releasing capacity of the dust particles used in our study. As a  
644 consequence, the addition of new nutrients from dust in our study and during the P and R DUNE

645 experiments were much higher, especially for NO<sub>x</sub>, than those observed by Pitta et al. (2017, and  
646 references therein) and Ridame et al. (2014) following the simulation of a dry Saharan dust  
647 deposition event. This confirms that wet dust deposition is a more efficient source of  
648 bioavailable nutrients ~~compared to~~ dry dust deposition.

649 Although NO<sub>x</sub> and DIP increases after dust addition were ~~rather similar during our three~~  
650 experiments, the subsequent dynamics of these elements and the impacts on plankton community  
651 composition and functioning were drastically different. While NO<sub>x</sub> levels decreased moderately  
652 over the course of our experiments due to biological uptake, more abrupt decreases were  
653 observed for DIP released by dust, reaching values close to the ones observed in the controls,  
654 except at station FAST where concentrations were still above ambient levels at the end of the  
655 experiment.

656 ~~Regarding biological stocks, most~~ experiments ~~reporting~~ on the effect of dust addition in  
657 the Mediterranean Sea showed significant increases in chlorophyll *a* concentrations (mean ~90%  
658 increase; Guieu and Ridame, 2020). Interestingly, no stimulation of autotrophic biomass and  
659 primary production rates (Gazeau et al., 2021) was observed in dust-amended tanks under  
660 present conditions at station TYR. To the best of our knowledge, this is the first experimental  
661 evidence of a complete absence of response from an autotrophic community following dust wet  
662 deposition. The absence of response from autotrophic stocks could be due to a tight top-down  
663 control ~~from~~ grazers hiding potential responses from the autotrophic community (Lekunberri et  
664 al., 2010; Marañón et al., 2010) and/or a competition for ~~nutritive resources~~ with heterotrophic  
665 prokaryotes (Marañón et al., 2010). ~~Regarding the first hypothesis,~~ Feliú et al. (2020) have  
666 shown that the mesozooplankton assemblage at TYR was clearly impacted by a dust event that  
667 took place nine days before sampling at that station as evidenced from particulate inventory of  
668 lithogenic proxies (Al, Fe) in the water column (Bressac et al., in preparation). This dust  
669 deposition likely stimulated phytoplankton growth and consequently **increased the abundance of**

670 herbivorous grazers (copepods) and attracted carnivorous species. ~~With respect to the second~~  
671 ~~hypothesis, it is well known that not only phytoplankton but also~~ heterotrophic bacteria are  
672 limited by inorganic nutrients, mainly DIP, in oligotrophic systems (Obernosterer et al., 2003;  
673 Van Wambeke et al., 2001). ~~Indeed, many~~ recent studies have shown significant increase in  
674 heterotrophic bacterial abundance, respiration and/or production following dust deposition (and  
675 nutrient enrichment) in these areas (Lekunberri et al., 2010; Pitta et al., 2017; Pulido-Villena et  
676 al., 2008; Romero et al., 2011). ~~Most of the time,~~ heterotrophic ~~processes~~ appear to be more  
677 stimulated ~~by dust pulses compared to~~ autotrophic ~~processes~~ with increasing degree of  
678 oligotrophy, ~~the dominant response being~~ modulated by the competition for nutrients between  
679 phytoplankton and bacteria (Marañón et al., 2010). This ~~is clearly what was observed at this~~  
680 station, with heterotrophic prokaryotes reacting quickly and strongly to nutrient addition both in  
681 terms of abundances and production rates (Gazeau et al., 2021). These two aforementioned  
682 hypotheses are not mutually exclusive, and the quick response of heterotrophic prokaryotes to  
683 dust addition is coherent with the ~~strongest~~ net heterotrophy ~~of the tested waters~~ at this station  
684 (see 4.1). ~~The strong stimulation of heterotrophic prokaryotes and the absence of detectable~~  
685 ~~effects on the autotrophic compartment drove the community towards an even stronger net~~  
686 ~~heterotrophic state as illustrated by the decrease in the autotrophic to heterotrophic biomass ratio~~  
687 ~~following dust addition (data not shown). This was further shown by~~ increases in community  
688 respiration and decreases in net community production rates in dust-amended as compared to  
689 control tanks (Gazeau et al., 2021) ~~and suggest that~~ dust addition to surface waters strongly  
690 dominated by heterotrophs leads to a reduction of the capacity of these ~~waters~~ to export organic  
691 matter and sequester atmospheric CO<sub>2</sub>.

692 In contrast to ~~what was observed~~ at TYR, ~~fertilization~~ of primary producers was observed at  
693 stations ION and FAST under present conditions with overall ~~relative changes much~~ higher ~~than~~  
694 ~~from~~ previous studies compiled by Guieu and Ridame (2020). The largest increase in chlorophyll



695 *a* concentrations at station FAST is coherent with the largest NO<sub>x</sub> decrease observed in our  
696 study, which occurred at this station. Interestingly, following dust addition at this station,  
697 autotrophic production did not lead to DIP exhaustion throughout the experiment as DIP  
698 concentrations were still above ambient conditions at the end of the experiment. Maximal  
699 primary production rates (<sup>14</sup>C-incorporation) at this station at the end of the experiment suggest a  
700 strong DIP recycling and the dominance of regenerated production towards the end of the  
701 experiment (Gazeau et al., 2021). Although, in some cases, *Synechococcus* appeared stimulated  
702 by dust addition (Herut et al., 2005; Lagaria et al., 2017; Paytan et al., 2009), Guieu et al.  
703 (2014b) showed that, based on the analysis of several aerosols addition studies, this group had  
704 generally weak responses to aerosol addition in contrast to nano- and micro-phytoplankton,  
705 suggesting that aerosol deposition may lead to an increase in larger size-class phytoplankton.  
706 Yet, at stations ION and FAST, the increase in *Synechococcus* abundance in dust-amended tanks  
707 was the highest relative to those of pico- and nano-eukaryotes. This was especially true at station  
708 ION where no clear response to nutrient enrichment was observed for nano-eukaryotes  
709 throughout the experiment. However, it must be stressed that our experiments were performed  
710 over a relatively short period (3 to 4 days), and the sharp increase in Fucoxanthin paralleled by a  
711 decrease in silicates, at the end of the experiment at station FAST where DIP limitation was not  
712 yet apparent, suggests a delayed response of diatoms as compared to smaller groups (i.e.  
713 autotrophic prokaryotes, pico- and nano-eukaryotes). Although this was not observed based on  
714 pigment analyses, the sharp decline in nano-eukaryote abundances in dust-amended tanks at the  
715 end of the FAST experiment, further suggests that this group, reacting quickly to nutrient  
716 enrichment was progressively grazed and/or outcompeted by larger phytoplankton species.

717 In contrast to what was observed at TYR, at station FAST, the competition for nutrients  
718 between autotrophs and heterotrophs was clearly in favor of autotrophs with a clear increase in  
719 the ratio between autotrophic and heterotrophic biomass reaching values of up to 4 (data not

720 shown). While, ~~as discussed above,~~ all groups of primary producers benefited from nutrient  
721 enrichment at ~~this station,~~ the increases in heterotrophic prokaryote abundances were rather  
722 ~~limited following dust deposition,~~ leading to an increase of net community production rates  
723 throughout this experiment ~~to reach~~ positive levels while control tanks remained below  
724 metabolic balance (Gazeau et al., 2021). At station ION, the situation was ~~somewhat~~  
725 intermediate with a similar enhancement of both autotrophic and heterotrophic stocks and no  
726 clear changes in the ratio between autotrophic and heterotrophic biomass (data not shown),  
727 although the system ~~appeared in favor of~~ net autotrophy at the end of the experiment in dust -  
728 amended tanks under present environmental conditions (Gazeau et al., 2021).

729         Transfer of newly produced organic matter to higher trophic levels in the different  
730 treatments was ~~evaluated~~ through the quantification of meso-zooplankton abundance at the end  
731 of each experiment. ~~Although we are fully aware that such an approach is certainly criticizable~~  
732 ~~considering the low incubation times (3 to 4 days), it may still be representative of lowered~~  
733 ~~mortality or faster growth.~~ Altogether it ~~does not appear as a surprise~~ that an increase in meso-  
734 zooplankton abundances was only detected at station FAST where the strongest enhancement of  
735 primary production was observed. Such an increase in meso-zooplankton abundance in the dust-  
736 amended as compared to control treatment was observed during land-based mesocosm  
737 experiments in the Eastern Mediterranean Sea (Pitta et al., 2017).

738         Finally, although no clear effects of dust deposition under present conditions were  
739 detectable on autotrophic prokaryotes at station TYR, the strongest increase in N<sub>2</sub> fixation rates  
740 was recorded at this station (Céline Ridame, unpublished results). However, the potential impact  
741 of this process on NO<sub>x</sub> concentration is ~~highly~~ negligible compared to the very large stock of  
742 NO<sub>x</sub> present in the dust-amended tanks, as less than 1 nmol L<sup>-1</sup> d<sup>-1</sup> of NO<sub>x</sub> ~~can be produced by~~  
743 ~~this process~~ (Céline Ridame, unpublished results).

## 744 **4.4. Impact of dust addition under future environmental** 745 **conditions**

746 ~~Very few past~~ studies have investigated the release and fate of nutrients from atmospheric  
747 ~~particles~~ under climate conditions as expected for the end of the century, and, to the best of our  
748 knowledge, our study represents the first attempt to test for the combined effect of ocean  
749 warming and acidification on these processes. ~~Louis et al. (2018) have already shown from an~~  
750 ~~experiment performed under close to abiotic conditions (seawater filtration onto 0.2 µm)~~ that  
751 even an extreme ocean acidification scenario (~ -0.6 pH units) does not impact the bioavailability  
752 of macro- and micro-nutrients (NO<sub>x</sub>, DIP and DFe) ~~from dust addition for surface phytoplankton~~  
753 ~~communities~~ in the oligotrophic Northwestern Mediterranean Sea, ~~using the same dust analog~~  
754 ~~and simulated flux as used during our experiments~~. Similar results were presented by Mélançon  
755 et al. (2016) ~~regarding the release of DFe from dust~~ in high-nutrient low-chlorophyll (HNLC)  
756 waters of the Northeastern Pacific, ~~following a mild~~ ocean acidification scenario of -0.2 pH  
757 units. As no differences were observed for NO<sub>x</sub> and DIP concentrations within few hours  
758 following dust addition under present and future environmental conditions, our results agree with  
759 these previous findings and further highlights the absence of direct effect of ocean warming (+3  
760 °C) on the release of nutrients from atmospheric particles.

761 In contrast, ~~following these similar nutrient releases,~~ different nutrient consumption  
762 dynamics were observed between ambient and warmed/acidified tanks. ~~These differences were~~  
763 ~~substantially dependent on the considered nutrient and investigated station. Regarding NO<sub>x</sub>,~~ no  
764 impacts of warming and acidification could be observed at stations TYR and ION due to low net  
765 ~~decreasing~~ rates compared to the large increase following dust addition. In contrast, at the most  
766 productive station FAST, as a consequence of strongly enhanced biological stocks (~~see~~

767 thereafter) and metabolic rates (Gazeau et al., 2021): larger NO<sub>x</sub> consumption rates were shown  
768 under future environmental conditions.

769 The differences in DIP dynamics between the two dust-amended treatments were more  
770 complex to interpret ~~depending on the investigated station~~. A clear feature of our experiments is  
771 that, in contrast to present day pH and temperature conditions, all the stock of DIP released from  
772 dust was consumed at the end of the three experiments under future conditions, ~~suggesting a~~  
773 ~~much faster consumption by autotrophs and heterotrophic prokaryotes~~. That being said, the rate  
774 of decrease ~~under future environmental conditions~~ differed depending on the station. While DIP  
775 dynamics were quite similar between tanks maintained under present and future environmental  
776 conditions at ION, warming and acidification induced a faster decrease of DIP at TYR and  
777 FAST, with a full consumption of the released DIP within 24 h. An interesting outcome at station  
778 TYR was that, despite the important discrepancies observed for autotrophic stocks and metabolic  
779 rates between the duplicates G1 and G2 (see section 4.2), a ~~very~~ similar dynamics was observed  
780 for DIP concentrations in these tanks. As heterotrophic prokaryote biomass and production rates  
781 (Gazeau et al., 2021) did not differ between these duplicate tanks, this further highlights the clear  
782 dominance of heterotrophic processes at this station, a dominance which was exacerbated by dust  
783 addition under future environmental conditions, leading to an even stronger heterotrophic state at  
784 the end of this experiment (Gazeau et al., 2021).

785 At station ION, large impacts of warming and acidification ~~have been observed~~,  
786 ~~especially for primary producers, as shown by almost doubled~~ chlorophyll *a* concentrations ~~as~~  
787 ~~compared to~~ dust amended tanks (D). At this station, all autotrophic groups ~~benefited from~~ ocean  
788 acidification and warming. *Synechococcus* and to a lesser extent pico-eukaryotes ~~appeared as the~~  
789 ~~most impacted ones~~. Yet these differences ~~of sensitivity among autotrophs~~ did not lead to  
790 ~~detectable~~ changes in the composition of the autotrophic assemblage ~~as compared to ambient~~  
791 ~~conditions~~, with ~~still a large dominance of~~ nano-eukaryote carbon biomass at the end of this

792 experiment (62% in treatment G vs. 64% in treatment D). ~~Interestingly,~~ although the ratio  
793 between autotrophic and heterotrophic biomass appeared ~~impacted positively~~ under future  
794 environmental conditions, reaching values of up to 2 at the end of ~~this~~ experiment (~~data not~~  
795 ~~shown~~), warming and acidification led to a decrease in net community production (Gazeau et al.,  
796 2021) suggesting that in the coming decades the capacity of surface seawater to sequester  
797 anthropogenic CO<sub>2</sub> will be lowered.

798 Similarly, at FAST, all phytoplankton groups were impacted positively by warming and  
799 acidification with the strongest changes detected for *Synechococcus* as compared to present  
800 environmental conditions. However, in contrast to station ION, all groups reached maximal  
801 abundances (and carbon biomass) after 3 days of incubations, thereafter drastically decreasing  
802 most likely as a consequence of DIP limitation (see above). It must be stressed that this pattern  
803 could not be observed ~~through pigment dynamics~~ as no ~~sampling was performed~~ for these  
804 analyses after 3 days of incubation. Also, in contrast to station ION, the abundance of  
805 heterotrophic prokaryotes in the warmer and acidified treatment reached a maximum after 2 days  
806 of incubations and then ~~strongly~~ decreased to reach levels observed in the control treatment. This  
807 suggests that ~~the heterotrophic compartment was~~ the first to suffer from DIP limitation and  
808 further highlights the dominance of ~~the autotrophic compartment~~ in terms of nutrient  
809 consumption at this station. ~~As observed at station ION,~~ although the ratio between autotrophic  
810 and heterotrophic biomass increased under future environmental conditions, Gazeau et al. (2021)  
811 reported on a decrease in net community production rates in this treatment as compared to  
812 ambient environmental conditions, suggesting that, in the future, nutrient release from dust will  
813 lead to a lesser sequestration capacity of surface waters for atmospheric CO<sub>2</sub>.

814 These positive effects of warming and acidification on the abundance of phytoplankton ~~cells,~~  
815 ~~especially for small species,~~ as observed at ION and FAST are in line with previously published  
816 studies. ~~Indeed, although very contrasted results have been shown on~~ the effect of ocean

817 acidification on small autotrophic species (e.g. Dutkiewicz et al., 2015), there is increasing  
818 evidence that small phytoplankton species will be favored in a warmer ocean (e.g. Chen et al.,  
819 2014; Daufresne et al., 2009; Morán et al., 2010). ~~As mentioned earlier,~~ our experimental  
820 protocol was not conceived to discriminate temperature from pH effects, however results concur  
821 with those of Maugendre et al. (2015) which further suggested temperature over elevated CO<sub>2</sub> as  
822 the main driver of increased picophytoplankton abundance in the Mediterranean Sea.

823         These enhanced fertilizing effects on primary producers at ION and FAST, under future  
824 as compared to present environmental conditions, did not seem to reach higher trophic levels as  
825 no clear differences in meso-zooplankton abundances were observed between ambient and  
826 warmed/acidified tanks at the end of the experiments. ~~We fully acknowledge that~~ the duration of  
827 our experiments was ~~certainly~~ too short to carefully assess the proportion of newly formed  
828 organic matter consumed by meso-zooplankton species and its effect on their abundances, yet  
829 group-specific variations were observed. ~~Similarly,~~ Gazeau et al. (2021) did not observe an  
830 additional impact of future environmental conditions on the export of organic matter after dust  
831 addition.

## 832 5. Conclusion

833 These experiments conducted during the PEACETIME cruise represent the first attempt  
834 to investigate the impacts of atmospheric deposition on surface plankton communities both under  
835 present and future environmental conditions. Despite few experimental issues ~~that are discussed~~,  
836 the three experiments provided new insights on these potential impacts in the open  
837 Mediterranean Sea. ~~Interestingly, the effect of dust deposition was highly different~~ between the  
838 three investigated stations in the Tyrrhenian Sea, Ionian Sea and in the Algerian basin. ~~As the~~  
839 initial conditions ~~in the sampled surface seawater~~ at the three stations were very similar in terms  
840 of nutrient ~~availability~~ and chlorophyll ~~content~~, these differences ~~rather~~ seem to be a  
841 consequence of the initial metabolic states of the community (autotrophy vs. heterotrophy). In all  
842 three cases, nutrient addition from dust deposition did not strongly modify but rather exacerbated  
843 this initial state. Relative changes in main parameters presented in this manuscript and processes  
844 presented in Gazeau et al. (2021) as a consequence of dust addition under present and future  
845 environmental conditions are shown in Fig. 10, and compared to the compilation of published  
846 data for the Mediterranean Sea from Guieu and Ridame (2020). At station TYR, under  
847 conditions of a clear dominance of heterotrophs on the use of resources and potentially a higher  
848 top-down control from grazers, dust addition drove the community into an even more  
849 heterotrophic state with no detectable effect on primary producers. At station ION, where the  
850 community was initially closer to metabolic balance, both heterotrophic and autotrophic  
851 compartments benefited from dust derived nutrients. At FAST, the ~~most active~~ station ~~in terms~~  
852 ~~of~~ autotrophic production, addition of nutrients ~~boosted~~ both compartments but heterotrophic  
853 prokaryotes became quickly P-limited and overall larger effects were observed for  
854 phytoplankton. Ocean acidification and warming did not have any detectable impact on the  
855 release of nutrients from atmospheric particles. Furthermore, these external drivers did not

856 drastically modify the composition of the autotrophic assemblage with all groups benefiting from  
857 warmer and acidified conditions. However, although for two out of the three stations  
858 investigated, larger increases were observed for autotrophic as compared to heterotrophic stocks  
859 under future environmental conditions, a stronger impact of warming and acidification on  
860 mineralization processes (Gazeau et al., 2021) suggests that, in the future, the plankton  
861 communities of Mediterranean surface waters will have a decreased capacity to sequester  
862 atmospheric CO<sub>2</sub> following the deposition of atmospheric particles.



## 863 **Data availability**

864 All data and metadata will be made available at the French INSU/CNRS LEFE CYBER database  
865 (scientific coordinator: Hervé Claustre; data manager, webmaster: Catherine Schmechtig).  
866 INSU/CNRS LEFE CYBER (2020)

## 867 **Author contributions**

868 FG and CG designed and supervised the study. FG, CG, CR and KD sampled seawater from the  
869 experimental tanks during the experiments. JMG and GDL participated in the technical  
870 preparation of the experimental system and all authors participated in sample analyses. FG, CR  
871 and CG wrote the paper with contributions from all authors.

## 872 **Financial support**

873 This study is a contribution to the PEACETIME project (<http://peacetime-project.org>), a joint  
874 initiative of the MERMEX and ChArMEX components supported by CNRS-INSU, IFREMER,  
875 CEA, and Météo-France as part of the programme MISTRALS coordinated by INSU.  
876 PEACETIME is a contribution to SOLAS and IMBER international programme. The project was  
877 endorsed as a process study by GEOTRACES. PEACETIME cruise  
878 (<https://doi.org/10.17600/17000300>). The project leading to this publication has also received  
879 funding from the European FEDER Fund under project 1166-39417.

## 880 **Acknowledgments**

881 The authors thank the captain and the crew of the RV Pourquoi Pas ? for their professionalism  
882 and their work at sea. We thank Julia Uitz, Céline Dimier and the SAPIGH HPLC analytical  
883 service at Institut de la Mer de Villefranche (IMEV) for sampling and analysis of phytoplankton  
884 pigments, John Dolan for microscopic countings as well as Lynne Macarez and the PIQv-

885 platform of EMBRC-France, a national Research Infrastructure supported by ANR, under the  
886 reference ANR-10-INSB-02, for mesozooplankton analyses.

## 887 **References**

- 888 Aminot, A. and K erouel, R.: Dosage automatique des nutriments dans les eaux marines :  
889 m ethodes en flux continu, Editions Ifremer, m ethodes d'analyse en milieu marin., 2007.
- 890 Behrenfeld, M. J., O'Malley, R. T., Siegel, D. A., McClain, C. R., Sarmiento, J. L., Feldman, G.  
891 C., Milligan, A. J., Falkowski, P. G., Letelier, R. M. and Boss, E. S.: Climate-driven trends  
892 in contemporary ocean productivity, *Nature*, 444(7120), 752–755, 2006.
- 893 Bergametti, Gi., Dutot, A.-L., Buat-M enard, P., Losno, R. and Remoudaki, E.: Seasonal  
894 variability of the elemental composition of atmospheric aerosol particles over the  
895 Northwestern Mediterranean, *Tellus B: Chemical and Physical Meteorology*, 41(3), 353–  
896 361, <https://doi.org/10.3402/tellusb.v41i3.15092>, 1989.
- 897 Bonnet, S. and Guieu, C.: Atmospheric forcing on the annual iron cycle in the western  
898 Mediterranean Sea: A 1-year survey, *Journal of Geophysical Research: Oceans*, 111(C9),  
899 <https://doi.org/10.1029/2005JC003213>, 2006.
- 900 Bonnet, S., Guieu, C., Chiaverini, J., Ras, J. and Stock, A.: Effect of atmospheric nutrients on the  
901 autotrophic communities in a low nutrient, low chlorophyll system, *Limnology and*  
902 *Oceanography*, 50(6), 1810–1819, <https://doi.org/10.4319/lo.2005.50.6.1810>, 2005.
- 903 B rsheim, K. Y. and Bratbak, G.: Cell volume to cell carbon conversion factors for a  
904 bacterivorous *Monas* sp. enriched from seawater, *Marine Ecology Progress Series*, 36(2),  
905 171–175, 1987.
- 906 Bosc, E., Bricaud, A. and Antoine, D.: Seasonal and interannual variability in algal biomass and  
907 primary production in the Mediterranean Sea, as derived from 4 years of SeaWiFS  
908 observations, *Global Biogeochemical Cycles*, 18(1),  
909 <https://doi.org/10.1029/2003GB002034>, 2004.
- 910 Bressac, M. and Guieu, C.: Post-depositional processes: What really happens to new atmospheric  
911 iron in the ocean's surface?, *Global Biogeochemical Cycles*, 27(3), 859–870,  
912 <https://doi.org/10.1002/gbc.20076>, 2013.

913 Bressac, M., Wagener, T., Tovar-Sanchez, A., Ridame, C., Albani, S., Fu, F., Desboeufs, K. and  
914 Guieu, C.: Residence time of dissolved and particulate trace elements in the surface  
915 Mediterranean Sea (Peacetime cruise), *Biogeosciences*, in preparation.

916 Bressac, M., Guieu, C., Doxaran, D., Bourrin, F., Desboeufs, K., Leblond, N. and Ridame, C.:  
917 Quantification of the lithogenic carbon pump following a simulated dust-deposition event  
918 in large mesocosms, *Biogeosciences*, 11(4), 1007–1020, [https://doi.org/10.5194/bg-11-](https://doi.org/10.5194/bg-11-1007-2014)  
919 1007-2014, 2014.

920 Chen, B., Liu, H., Huang, B. and Wang, J.: Temperature effects on the growth rate of marine  
921 picoplankton, *Marine Ecology Progress Series*, 505, 37–47,  
922 <https://doi.org/10.3354/meps10773>, 2014.

923 Christaki, U., Courties, C., Massana, R., Catala, P., Lebaron, P., Gasol, J. M. and Zubkov, M. V.:  
924 Optimized routine flow cytometric enumeration of heterotrophic flagellates using SYBR  
925 Green I, *Limnology and Oceanography: Methods*, 9(8), 329–339,  
926 <https://doi.org/10.4319/lom.2011.9.329>, 2011.

927 Daufresne, M., Lengfellner, K. and Sommer, U.: Global warming benefits the small in aquatic  
928 ecosystems, *PNAS*, 106(31), 12788–12793, <https://doi.org/10.1073/pnas.0902080106>,  
929 2009.

930 Desboeufs, K., Leblond, N., Wagener, T., Bon Nguyen, E. and Guieu, C.: Chemical fate and  
931 settling of mineral dust in surface seawater after atmospheric deposition observed from  
932 dust seeding experiments in large mesocosms, *Biogeosciences*, 11(19), 5581–5594,  
933 <https://doi.org/10.5194/bg-11-5581-2014>, 2014.

934 Desboeufs, K., Bon Nguyen, E., Chevaillier, S., Triquet, S. and Dulac, F.: Fluxes and sources of  
935 nutrient and trace metal atmospheric deposition in the Northwestern Mediterranean,  
936 *Atmospheric Chemistry and Physics*, 18(19), 14477–14492, [https://doi.org/10.5194/acp-](https://doi.org/10.5194/acp-18-14477-2018)  
937 18-14477-2018, 2018.

938 Dickson, A. G., Sabine, C. L. and Christian, J. R.: Guide to best practices for ocean CO<sub>2</sub>  
939 measurements, PICES, Sydney., 2007.

940 Dinasquet, J., Bigeard, E., Gazeau, F., Marañón, E., Ridame, C., Van Wambeke, F.,  
941 Obernosterer, I. and Baudoux, A.-C.: Impact of dust enrichment on the microbial food web  
942 under present and future conditions of pH and temperature, *Biogeosciences Discussions*,  
943 2021.

944 Djaoudi, K., Van Wambeke, F., Coppola, L., D’Ortenzio, F., Helias-Nunige, S., Raimbault, P.,  
945 Taillandier, V., Testor, P., Wagener, T. and Pulido-Villena, E.: Sensitive Determination of  
946 the Dissolved Phosphate Pool for an Improved Resolution of Its Vertical Variability in the  
947 Surface Layer: New Views in the P-Depleted Mediterranean Sea, *Front. Mar. Sci.*, 5,  
948 <https://doi.org/10.3389/fmars.2018.00234>, 2018.

949 D’Ortenzio, F., Iudicone, D., Montegut, C. de B., Testor, P., Antoine, D., Marullo, S., Santoleri,  
950 R. and Madec, G.: Seasonal variability of the mixed layer depth in the Mediterranean Sea  
951 as derived from in situ profiles, *Geophysical Research Letters*, 32(12),  
952 <https://doi.org/10.1029/2005GL022463>, 2005.

953 Duce, R. A., Liss, P. S., Merrill, J. T., Atlas, E. L., Buat-Menard, P., Hicks, B. B., Miller, J. M.,  
954 Prospero, J. M., Arimoto, R., Church, T. M., Ellis, W., Galloway, J. N., Hansen, L.,  
955 Jickells, T. D., Knap, A. H., Reinhardt, K. H., Schneider, B., Soudine, A., Tokos, J. J.,  
956 Tsunogai, S., Wollast, R. and Zhou, M.: The atmospheric input of trace species to the  
957 world ocean, *Global Biogeochemical Cycles*, 5(3), 193–259,  
958 <https://doi.org/10.1029/91GB01778>, 1991.

959 Dutkiewicz, S., Morris, J. J., Follows, M. J., Scott, J., Levitan, O., Dyhrman, S. T. and Berman-  
960 Frank, I.: Impact of ocean acidification on the structure of future phytoplankton  
961 communities, *Nature Climate change*, 5, 1002–1006, <https://doi.org/10.1038/nclimate2722>,  
962 2015.

963 Emerson, S., Quay, P., Karl, D., Winn, C., Tupas, L. and Landry, M.: Experimental  
964 determination of the organic carbon flux from open-ocean surface waters, *Nature*,  
965 389(6654), 951–954, <https://doi.org/10.1038/40111>, 1997.

966 Falkovich, A. H., Ganor, E., Levin, Z., Formenti, P. and Rudich, Y.: Chemical and mineralogical  
967 analysis of individual mineral dust particles, *Journal of Geophysical Research:*  
968 *Atmospheres*, 106(D16), 18029–18036, <https://doi.org/10.1029/2000JD900430>, 2001.

969 Feliú, G., Pagano, M., Hidalgo, P. and Carlotti, F.: Structure and function of epipelagic  
970 mesozooplankton and their response to dust deposition events during the spring  
971 PEACETIME cruise in the Mediterranean Sea, *Biogeosciences*, 17, 5417–5441,  
972 <https://doi.org/10.5194/bg-17-5417-2020>, 2020.

973 Gazeau, F., Van Wambeke, F., Marañón, E., Pérez-Lorenzo, M., Alliouane, S., Stolpe, C.,  
974 Blasco, T., Leblond, N., Zäncker, B., Engel, A., Marie, B., Dinasquet, J. and Guieu, C.:  
975 Impact of dust addition on the metabolism of Mediterranean plankton communities and  
976 carbon export under present and future conditions of pH and temperature, *Biogeosciences*  
977 *Discussions*, 2021.

978 Giovagnetti, V., Brunet, C., Conversano, F., Tramontano, F., Obernosterer, I., Ridame, C. and  
979 Guieu, C.: Assessing the role of dust deposition on phytoplankton ecophysiology and  
980 succession in a low-nutrient low-chlorophyll ecosystem: a mesocosm experiment in the  
981 Mediterranean Sea, *Biogeosciences*, 10(5), 2973–2991, [https://doi.org/10.5194/bg-10-](https://doi.org/10.5194/bg-10-2973-2013)  
982 [2973-2013](https://doi.org/10.5194/bg-10-2973-2013), 2013.

983 Gorsky, G., Ohman, M. D., Picheral, M., Gasparini, S., Stemmann, L., Romagnan, J.-B.,  
984 Cawood, A., Pesant, S., García-Comas, C. and Prejger, F.: Digital zooplankton image  
985 analysis using the ZooScan integrated system, *J Plankton Res*, 32(3), 285–303,  
986 <https://doi.org/10.1093/plankt/fbp124>, 2010.

987 Guieu, C. and Ridame, C.: Impact of atmospheric deposition on marine chemistry and  
988 biogeochemistry, in *Atmospheric Chemistry in the Mediterranean Region: Comprehensive*

989           Diagnosis and Impacts, edited by F. Dulac, S. Sauvage, and E. Hamonou, Springer, Cham,  
990           Switzerland, , 2020.

991   Guieu, C., Dulac, F., Desboeufs, K., Wagener, T., Pulido-Villena, E., Grisoni, J.-M., Louis, F.,  
992           Ridame, C., Blain, S., Brunet, C., Bon Nguyen, E., Tran, S., Labiadh, M. and Dominici, J.-  
993           M.: Large clean mesocosms and simulated dust deposition: a new methodology to  
994           investigate responses of marine oligotrophic ecosystems to atmospheric inputs,  
995           Biogeosciences, 7(9), 2765–2784, <https://doi.org/10.5194/bg-7-2765-2010>, 2010a.

996   Guieu, C., Loye-Pilot, M. D., Benyahya, L. and Dufour, A.: Spatial variability of atmospheric  
997           fluxes of metals (Al, Fe, Cd, Zn and Pb) and phosphorus over the whole Mediterranean  
998           from a one-year monitoring experiment: Biogeochemical implications, Marine Chemistry,  
999           120(1–4), 164–178, <https://doi.org/10.1016/j.marchem.2009.02.004>, 2010b.

1000   Guieu, C., Ridame, C., Pulido-Villena, E., Bressac, M., Desboeufs, K. and Dulac, F.: Impact of  
1001           dust deposition on carbon budget: a tentative assessment from a mesocosm approach,  
1002           Biogeosciences, 11(19), 5621–5635, 2014a.

1003   Guieu, C., Aumont, O., Paytan, A., Bopp, L., Law, C. S., Mahowald, N., Achterberg, E. P.,  
1004           Marañón, E., Salihoglu, B., Crise, A., Wagener, T., Herut, B., Desboeufs, K., Kanakidou,  
1005           M., Olgun, N., Peters, F., Pulido-Villena, E., Tovar-Sanchez, A. and Völker, C.: The  
1006           significance of the episodic nature of atmospheric deposition to Low Nutrient Low  
1007           Chlorophyll regions, Global Biogeochemical Cycles, 28(11), 1179–1198,  
1008           <https://doi.org/10.1002/2014GB004852>, 2014b.

1009   Guieu, C., D’Ortenzio, F., Dulac, F., Taillandier, V., Doglioli, A., Petrenko, A., Barrillon, S.,  
1010           Mallet, M., Nabat, P. and Desboeufs, K.: Process studies at the air-sea interface after  
1011           atmospheric deposition in the Mediterranean Sea: objectives and strategy of the  
1012           PEACETIME oceanographic campaign (May–June 2017), Biogeosciences, 2020(17),  
1013           5563–5585, <https://doi.org/10.5194/bg-17-5563-2020>, 2020.

1014 Herut, B., Zohary, T., Krom, M. D., Mantoura, R. F. C., Pitta, P., Psarra, S., Rassoulzadegan, F.,  
1015 Tanaka, T. and Frede Thingstad, T.: Response of East Mediterranean surface water to  
1016 Saharan dust: On-board microcosm experiment and field observations, *Deep Sea Research*  
1017 *Part II: Topical Studies in Oceanography*, 52(22), 3024–3040,  
1018 <https://doi.org/10.1016/j.dsr2.2005.09.003>, 2005.

1019 Holmes, R. M., Aminot, A., K erouel, R., Hooker, B. A. and Peterson, B. J.: A simple and precise  
1020 method for measuring ammonium in marine and freshwater ecosystems, *Can. J. Fish.*  
1021 *Aquat. Sci.*, 56(10), 1801–1808, <https://doi.org/10.1139/f99-128>, 1999.

1022 IPCC: *Climate Change, The Physical Science Basis.*, 2013.

1023 IPCC: *IPCC Special Report on the Ocean and Cryosphere in a Changing Climate*, edited by H.  
1024 O. P rtner, D. C. Roberts, V. Masson-Delmotte, P. Zhai, M. Tignor, E. Poloczanska, K.  
1025 Mintenbeck, A. Alegr a, M. Nicolai, A. Okem, J. Petzold, B. Rama, and N. M. Weyer.,  
1026 2019.

1027 Irwin, A. J. and Oliver, M. J.: Are ocean deserts getting larger?, *Geophysical Research Letters*,  
1028 36, <https://doi.org/10.1029/2009gl039883>, 2009.

1029 Jickells, T. D., An, Z. S., Andersen, K. K., Baker, A. R., Bergametti, G., Brooks, N., Cao, J. J.,  
1030 Boyd, P. W., Duce, R. A., Hunter, K. A., Kawahata, H., Kubilay, N., laRoche, J., Liss, P.  
1031 S., Mahowald, N., Prospero, J. M., Ridgwell, A. J., Tegen, I. and Torres, R.: *Global Iron*  
1032 *Connections Between Desert Dust, Ocean Biogeochemistry, and Climate*, *Science*,  
1033 308(5718), 67–71, <https://doi.org/10.1126/science.1105959>, 2005.

1034 Kana, T. M. and Glibert, P. M.: Effect of irradiances up to 2000  $\mu\text{E m}^{-2} \text{ s}^{-1}$  on marine  
1035 *Synechococcus* WH7803—I. Growth, pigmentation, and cell composition, *Deep Sea*  
1036 *Research Part A. Oceanographic Research Papers*, 34(4), 479–495,  
1037 [https://doi.org/10.1016/0198-0149\(87\)90001-X](https://doi.org/10.1016/0198-0149(87)90001-X), 1987.



1038 Kapsenberg, L., Alliouane, S., Gazeau, F., Mousseau, L. and Gattuso, J.-P.: Coastal ocean  
1039 acidification and increasing total alkalinity in the northwestern Mediterranean Sea, *Ocean*  
1040 *Science*, 13, 411–426, <https://doi.org/10.5194/os-13-411-2017>, 2017.

1041 Kouvarakis, G., Mihalopoulos, N., Tselepides, A. and Stavrakakis, S.: On the importance of  
1042 atmospheric inputs of inorganic nitrogen species on the productivity of the Eastern  
1043 Mediterranean Sea, *Global Biogeochemical Cycles*, 15(4), 805–817,  
1044 <https://doi.org/10.1029/2001GB001399>, 2001.

1045 Lagaria, A., Mandalakis, M., Mara, P., Papageorgiou, N., Pitta, P., Tsiola, A., Kagiorgi, M. and  
1046 Psarra, S.: Phytoplankton response to Saharan dust depositions in the Eastern  
1047 Mediterranean Sea: A mesocosm study, *Front. Mar. Sci.*, 3,  
1048 <https://doi.org/10.3389/fmars.2016.00287>, 2017.

1049 Law, C. S., Brévière, E., de Leeuw, G., Garçon, V., Guieu, C., Kieber, D. J., Konradowitz, S.,  
1050 Paulmier, A., Quinn, P. K., Saltzman, E. S., Stefels, J. and von Glasow, R.: Evolving  
1051 research directions in Surface Ocean - Lower Atmosphere (SOLAS) science, *Environ.*  
1052 *Chem.*, 10(1), 1, <https://doi.org/10.1071/EN12159>, 2013.

1053 Lee, S. and Fuhrman, J. A.: Relationships between Biovolume and Biomass of Naturally Derived  
1054 Marine Bacterioplankton, *Appl Environ Microbiol*, 53(6), 1298–1303, 1987.

1055 Lekunberri, I., Lefort, T., Romero, E., Vázquez-Domínguez, E., Romera-Castillo, C., Marrasé,  
1056 C., Peters, F., Weinbauer, M. and Gasol, J. M.: Effects of a dust deposition event on  
1057 coastal marine microbial abundance and activity, bacterial community structure and  
1058 ecosystem function, *J Plankton Res*, 32(4), 381–396,  
1059 <https://doi.org/10.1093/plankt/fbp137>, 2010.

1060 Liu, X., Patsavas, M. C. and Byrne, R. H.: Purification and Characterization of meta-Cresol  
1061 Purple for Spectrophotometric Seawater pH Measurements, *Environ. Sci. Technol.*, 45(11),  
1062 4862–4868, <https://doi.org/10.1021/es200665d>, 2011.

1063 Longhurst, A., Sathyendranath, S., Platt, T. and Caverhill, C.: An estimate of global primary  
1064 production in the ocean from satellite radiometer data, *Journal of Plankton Research*, 17(6),  
1065 1245–1271, <https://doi.org/10.1093/plankt/17.6.1245>, 1995.

1066 López-Urrutia, A. and Morán, X. A. G.: Resource limitation of bacterial production distorts the  
1067 temperature dependence of oceanic carbon cycling, *Ecology*, 88(4), 817–822,  
1068 <https://doi.org/10.1890/06-1641>, 2007.

1069 Louis, J., Pedrotti, M. L., Gazeau, F. and Guieu, C.: Experimental evidence of formation of  
1070 transparent exopolymer particles (TEP) and POC export provoked by dust addition under  
1071 current and high  $p\text{CO}_2$  conditions, *PLOS ONE*, 12(2), e0171980,  
1072 <https://doi.org/10.1371/journal.pone.0171980>, 2017a.

1073 Louis, J., Guieu, C. and Gazeau, F.: Nutrient dynamics under different ocean acidification  
1074 scenarios in a low nutrient low chlorophyll system: The Northwestern Mediterranean Sea,  
1075 *Estuarine, Coastal and Shelf Science*, 186, 30–44,  
1076 <https://doi.org/10.1016/j.ecss.2016.01.015>, 2017b.

1077 Louis, J., Gazeau, F. and Guieu, C.: Atmospheric nutrients in seawater under current and high  
1078  $p\text{CO}_2$  conditions after Saharan dust deposition: Results from three minicosm experiments,  
1079 *Progress in Oceanography*, 163, 40–49, <https://doi.org/10.1016/j.pocean.2017.10.011>,  
1080 2018.

1081 Loÿe-Pilot, M. D. and Martin, J. M.: Saharan Dust Input to the Western Mediterranean: An  
1082 Eleven Years Record in Corsica, in *The Impact of Desert Dust Across the Mediterranean*,  
1083 edited by S. Guerzoni and R. Chester, pp. 191–199, Springer Netherlands, Dordrecht,  
1084 [https://doi.org/10.1007/978-94-017-3354-0\\_18](https://doi.org/10.1007/978-94-017-3354-0_18), , 1996.

1085 Manca, B., Burca, M., Giorgetti, A., Coatanoan, C., Garcia, M.-J. and Iona, A.: Physical and  
1086 biochemical averaged vertical profiles in the Mediterranean regions: an important tool to  
1087 trace the climatology of water masses and to validate incoming data from operational

1088 oceanography, *Journal of Marine Systems*, 48(1), 83–116,  
1089 <https://doi.org/10.1016/j.jmarsys.2003.11.025>, 2004.

1090 Marañón, E., Fernández, A., Mouriño-Carballido, B., Martínez-García, S., Teira, E., Cermeño,  
1091 P., Chouciño, P., Huete-Ortega, M., Fernández, E., Calvo-Díaz, A., Morán, X. A. G.,  
1092 Bode, A., Moreno-Ostos, E., Varela, M. M., Patey, M. D. and Achterberg, E. P.: Degree of  
1093 oligotrophy controls the response of microbial plankton to Saharan dust, *Limnology and*  
1094 *Oceanography*, 55(6), 2339–2352, <https://doi.org/10.4319/lo.2010.55.6.2339>, 2010.

1095 Marañón, E., Lorenzo, M. P., Cermeño, P. and Mouriño-Carballido, B.: Nutrient limitation  
1096 suppresses the temperature dependence of phytoplankton metabolic rates, *The ISME*  
1097 *Journal*, 12(7), 1836–1845, <https://doi.org/10.1038/s41396-018-0105-1>, 2018.

1098 Marie, D., Simon, N., Guillou, L., Partensky, F. and Vault, D.: Flow cytometry analysis of  
1099 marine picoplankton, in *living color: protocols in flow cytometry and cell sorting*, edited  
1100 by R. A. Diamond and S. DeMaggio, pp. 421–454, Springer, Berlin, , 2010.

1101 Markaki, Z., Oikonomou, K., Kocak, M., Kouvarakis, G., Chaniotaki, A., Kubilay, N. and  
1102 Mihalopoulos, N.: Atmospheric deposition of inorganic phosphorus in the Levantine Basin,  
1103 eastern Mediterranean: Spatial and temporal variability and its role in seawater  
1104 productivity, *Limnology and Oceanography*, 48(4), 1557–1568,  
1105 <https://doi.org/10.4319/lo.2003.48.4.1557>, 2003.

1106 Maugendre, L., Gattuso, J.-P., Louis, J., de Kluijver, A., Marro, S., Soetaert, K. and Gazeau, F.:  
1107 Effect of ocean warming and acidification on a plankton community in the NW  
1108 Mediterranean Sea, *ICES Journal of Marine Science*, 72(6), 1744–1755,  
1109 <https://doi.org/10.1093/icesjms/fsu161>, 2015.

1110 Maugendre, L., Guieu, C., Gattuso, J.-P. and Gazeau, F.: Ocean acidification in the  
1111 Mediterranean Sea: Pelagic mesocosm experiments. A synthesis, *Estuarine, Coastal and*  
1112 *Shelf Science*, 186, 1–10, <https://doi.org/10.1016/j.ecss.2017.01.006>, 2017.

1113 Mayot, N., D'Ortenzio, F., Ribera d'Alcalà, M., Lavigne, H. and Claustre, H.: Interannual  
1114 variability of the Mediterranean trophic regimes from ocean color satellites,  
1115 *Biogeosciences*, 13(6), 1901–1917, <https://doi.org/10.5194/bg-13-1901-2016>, 2016.

1116 Mélançon, J., Levasseur, M., Lizotte, M., Scarratt, M., Tremblay, J.-É., Tortell, P., Yang, G.-P.,  
1117 Shi, G.-Y., Gao, H., Semeniuk, D., Robert, M., Arychuk, M., Johnson, K., Sutherland, N.,  
1118 Davelaar, M., Nemcek, N., Peña, A. and Richardson, W.: Impact of ocean acidification on  
1119 phytoplankton assemblage, growth, and DMS production following Fe-dust additions in  
1120 the NE Pacific high-nutrient, low-chlorophyll waters, *Biogeosciences*, 13(5), 1677–1692,  
1121 <https://doi.org/10.5194/bg-13-1677-2016>, 2016.

1122 Moore, C. M., Mills, M. M., Arrigo, K. R., Berman-Frank, I., Bopp, L., Boyd, P. W., Galbraith,  
1123 E. D., Geider, R. J., Guieu, C., Jaccard, S. L., Jickells, T. D., La Roche, J., Lenton, T. M.,  
1124 Mahowald, N. M., Marañón, E., Marinov, I., Moore, J. K., Nakatsuka, T., Oschlies, A.,  
1125 Saito, M. A., Thingstad, T. F., Tsuda, A. and Ulloa, O.: Processes and patterns of oceanic  
1126 nutrient limitation, *Nature Geoscience*, 6(9), 701–710, <https://doi.org/10.1038/ngeo1765>,  
1127 2013.

1128 Morán, X. A. G., López-Urrutia, Á., Calvo-Díaz, A. and Li, W. K. W.: Increasing importance of  
1129 small phytoplankton in a warmer ocean, *Global Change Biology*, 16(3), 1137–1144,  
1130 <https://doi.org/10.1111/j.1365-2486.2009.01960.x>, 2010.

1131 Neale, P. J., Sobrino, C., Segovia, M., Mercado, J. M., Leon, P., Cortés, M. D., Tuite, P., Picazo,  
1132 A., Salles, S., Cabrerizo, M. J., Prasil, O., Montecino, V., Reul, A. and Fuentes-Lema, A.:  
1133 Effect of CO<sub>2</sub>, nutrients and light on coastal plankton. I. Abiotic conditions and biological  
1134 responses, *Aquatic Biology*, 22, 25–41, <https://doi.org/10.3354/ab00587>, 2014.

1135 Obernosterer, I., Kawasaki, N. and Benner, R.: P-limitation of respiration in the Sargasso Sea  
1136 and uncoupling of bacteria from P-regeneration in size-fractionation experiments, *Aquatic  
1137 Microbial Ecology*, 32(3), 229–237, <https://doi.org/10.3354/ame032229>, 2003.

1138 Orr, J. C., Epitalon, J.-M., Dickson, A. G. and Gattuso, J.-P.: Routine uncertainty propagation for  
1139 the marine carbon dioxide system, *Marine Chemistry*, 207, 84–107,  
1140 <https://doi.org/10.1016/j.marchem.2018.10.006>, 2018.

1141 Paytan, A., Mackey, K. R. M., Chen, Y., Lima, I. D., Doney, S. C., Mahowald, N., Labiosa, R.  
1142 and Post, A. F.: Toxicity of atmospheric aerosols on marine phytoplankton, *Proceedings of*  
1143 *the National Academy of Sciences*, 106(12), 4601–4605,  
1144 <https://doi.org/10.1073/pnas.0811486106>, 2009.

1145 Pitta, P., Kanakidou, M., Mihalopoulos, N., Christodoulaki, S., Dimitriou, P. D., Frangoulis, C.,  
1146 Giannakourou, A., Kagiorgi, M., Lagaria, A., Nikolaou, P., Papageorgiou, N., Psarra, S.,  
1147 Santi, I., Tsapakis, M., Tsiola, A., Violaki, K. and Petihakis, G.: Saharan Dust Deposition  
1148 Effects on the Microbial Food Web in the Eastern Mediterranean: A Study Based on a  
1149 Mesocosm Experiment, *Front. Mar. Sci.*, 4, <https://doi.org/10.3389/fmars.2017.00117>,  
1150 2017.

1151 Polovina, J. J., Howell, E. A. and Abecassis, M.: Ocean’s least productive waters are expanding,  
1152 *Geophysical Research Letters*, 35(3), <https://doi.org/10.1029/2007gl031745>, 2008.

1153 Powley, H. R., Krom, M. D. and Cappellen, P. V.: Understanding the unique biogeochemistry of  
1154 the Mediterranean Sea: Insights from a coupled phosphorus and nitrogen model, *Global*  
1155 *Biogeochemical Cycles*, 31(6), 1010–1031, <https://doi.org/10.1002/2017GB005648>, 2017.

1156 Pulido-Villena, E., Wagener, T. and Guieu, C.: Bacterial response to dust pulses in the western  
1157 Mediterranean: Implications for carbon cycling in the oligotrophic ocean, *Global*  
1158 *Biogeochemical Cycles*, 22(1), <https://doi.org/10.1029/2007gb003091>, 2008.

1159 Pulido-Villena, E., Rerolle, V. and Guieu, C.: Transient fertilizing effect of dust in P-deficient  
1160 LNLC surface ocean, *Geophysical Research Letters*, 37,  
1161 <https://doi.org/10.1029/2009gl041415>, 2010.

1162 Pulido-Villena, E., Baudoux, A.-C., Obernosterer, I., Landa, M., Caparros, J., Catala, P.,  
1163 Georges, C., Harmand, J. and Guieu, C.: Microbial food web dynamics in response to a

1164 Saharan dust event: results from a mesocosm study in the oligotrophic Mediterranean Sea,  
1165 Biogeosciences, 11(19), 5607–5619, 2014.

1166 Putaud, J.-P., Dingenen, R. V., Dell’Acqua, A., Raes, F., Matta, E., Decesari, S., Facchini, M. C.  
1167 and Fuzzi, S.: Size-segregated aerosol mass closure and chemical composition in Monte  
1168 Cimone (I) during MINATROC, Atmospheric Chemistry and Physics, 4(4), 889–902,  
1169 <https://doi.org/10.5194/acp-4-889-2004>, 2004.

1170 Ras, J., Claustre, H. and Uitz, J.: Spatial variability of phytoplankton pigment distributions in the  
1171 Subtropical South Pacific Ocean: comparison between in situ and predicted data,  
1172 Biogeosciences, 5(2), 353–369, <https://doi.org/10.5194/bg-5-353-2008>, 2008.

1173 Regaudie-de-Gioux, A., Vaquer-Sunyer, R. and Duarte, C. M.: Patterns in planktonic  
1174 metabolism in the Mediterranean Sea, Biogeosciences, 6(12), 3081–3089,  
1175 <https://doi.org/10.5194/bg-6-3081-2009>, 2009.

1176 Richon, C., Dutay, J.-C., Dulac, F., Wang, R., Balkanski, Y., Nabat, P., Aumont, O., Desboeufs,  
1177 K., Laurent, B., Guieu, C., Raimbault, P. and Beuvier, J.: Modeling the impacts of  
1178 atmospheric deposition of nitrogen and desert dust-derived phosphorus on nutrients and  
1179 biological budgets of the Mediterranean Sea, Progress in Oceanography, 163, 21–39,  
1180 <https://doi.org/10.1016/j.pocean.2017.04.009>, 2018.

1181 Ridame, C. and Guieu, C.: Saharan input of phosphate to the oligotrophic water of the open  
1182 western Mediterranean Sea, Limnology and Oceanography, 47(3), 856–869, 2002.

1183 Ridame, C., Guieu, C. and L’Helguen, S.: Strong stimulation of N<sub>2</sub> fixation in oligotrophic  
1184 Mediterranean Sea: results from dust addition in large in situ mesocosms, Biogeosciences,  
1185 10(11), 7333–7346, 2013.

1186 Ridame, C., Dekazemacker, J., Guieu, C., Bonnet, S., L’Helguen, S. and Malien, F.: Contrasted  
1187 Saharan dust events in LNLC environments: impact on nutrient dynamics and primary  
1188 production, Biogeosciences (BG), 11(17), 4783–4800, 2014.

1189 Romero, E., Peters, F., Marrasé, C., Guadayol, Ò., Gasol, J. M. and Weinbauer, M. G.: Coastal  
1190 Mediterranean plankton stimulation dynamics through a dust storm event: An experimental  
1191 simulation, *Estuarine, Coastal and Shelf Science*, 93(1), 27–39,  
1192 <https://doi.org/10.1016/j.ecss.2011.03.019>, 2011.

1193 Roy-Barman, M., Folio, L., Douville, E., Leblond, N., Gazeau, F., Bressac, M., Wagener, T.,  
1194 Ridame, C., Desboeufs, K. and Guieu, C.: Contrasted release of insoluble elements (Fe, Al,  
1195 REE, Th, Pa) after dust deposition in seawater: a tank experiment approach,  
1196 *Biogeosciences Discussions*, 1–27, <https://doi.org/10.5194/bg-2020-247>, 2020.

1197 Sala, M. M., Aparicio, F. L., Balagué, V., Boras, J. A., Borrull, E., Cardelús, C., Cros, L.,  
1198 Gomes, A., López-Sanz, A., Malits, A., Martínez, R. A., Mestre, M., Movilla, J., Sarmiento,  
1199 H., Vázquez-Domínguez, E., Vaqué, D., Pinhassi, J., Calbet, A., Calvo, E., Gasol, J. M.,  
1200 Pelejero, C. and Marrasé, C.: Contrasting effects of ocean acidification on the microbial  
1201 food web under different trophic conditions, *ICES Journal of Marine Science*, 73(3), 670–  
1202 679, <https://doi.org/10.1093/icesjms/fsv130>, 2016.

1203 Sherr, E. B. and Sherr, B. F.: Bacterivory and herbivory: Key roles of phagotrophic protists in  
1204 pelagic food webs, *Microb Ecol*, 28(2), 223–235, <https://doi.org/10.1007/BF00166812>,  
1205 1994.

1206 Siokou-Frangou, I., Christaki, U., Mazzocchi, M. G., Montresor, M., Ribera d'Alcalá, M.,  
1207 Vaqué, D. and Zingone, A.: Plankton in the open Mediterranean Sea: a review,  
1208 *Biogeosciences*, 7(5), 1543–1586, <https://doi.org/10.5194/bg-7-1543-2010>, 2010.

1209 Tanaka, T., Thingstad, T. F., Christaki, U., Colombet, J., Cornet-Barthaux, V., Courties, C.,  
1210 Grattepanche, J.-D., Lagaria, A., Nedoma, J., Oriol, L., Psarra, S., Pujo-Pay, M. and  
1211 Wambeke, F. V.: Lack of P-limitation of phytoplankton and heterotrophic prokaryotes in  
1212 surface waters of three anticyclonic eddies in the stratified Mediterranean Sea,  
1213 *Biogeosciences*, 8(2), 525–538, <https://doi.org/10.5194/bg-8-525-2011>, 2011.

1214 Ternon, E., Guieu, C., Loÿe-Pilot, M.-D., Leblond, N., Bosc, E., Gasser, B., Miquel, J.-C. and  
1215 Martín, J.: The impact of Saharan dust on the particulate export in the water column of the  
1216 North Western Mediterranean Sea, *Biogeosciences*, 7(3), 809–826,  
1217 <https://doi.org/10.5194/bg-7-809-2010>, 2010.

1218 The Mermex group: Marine ecosystems' responses to climatic and anthropogenic forcings in the  
1219 Mediterranean, *Progress in Oceanography*, 91(2), 97–166,  
1220 <https://doi.org/10.1016/j.pocean.2011.02.003>, 2011.

1221 Theodosi, C., Markaki, Z., Tselepides, A. and Mihalopoulos, N.: The significance of atmospheric  
1222 inputs of soluble and particulate major and trace metals to the eastern Mediterranean  
1223 seawater, *Marine Chemistry*, 120(1), 154–163,  
1224 <https://doi.org/10.1016/j.marchem.2010.02.003>, 2010.

1225 Van Wambeke, F., Goutx, M., Striby, L., Sempéré, R. and Vidussi, F.: Bacterial dynamics  
1226 during the transition from spring bloom to oligotrophy in the northwestern Mediterranean  
1227 Sea: relationships with particulate detritus and dissolved organic matter, *Marine Ecology*  
1228 *Progress Series*, 212, 89–105, 2001.

1229 Van Wambeke, F., Taillandier, V., Deboeufs, K., Pulido-Villena, E., Dinasquet, J., Engel, A.,  
1230 Marañón, E., Ridame, C. and Guieu, C.: Influence of atmospheric deposition on  
1231 biogeochemical cycles in an oligotrophic ocean system, *Biogeosciences Discussions*, 1–51,  
1232 <https://doi.org/10.5194/bg-2020-411>, 2020a.

1233 Van Wambeke, F., Pulido, E., Dinasquet, J., Djaoudi, K., Engel, A., Garel, M., Guasco, S.,  
1234 Nunige, S., Taillandier, V., Zäncker, B. and Tamburini, C.: Spatial patterns of biphasic  
1235 ectoenzymatic kinetics related to biogeochemical properties in the Mediterranean Sea,  
1236 *Biogeosciences Discussions*, 1–38, <https://doi.org/10.5194/bg-2020-253>, 2020b.

1237 Verity, P. G., Robertson, C. Y., Tronzo, C. R., Andrews, M. G., Nelson, J. R. and Sieracki, M.  
1238 E.: Relationships between cell volume and the carbon and nitrogen content of marine

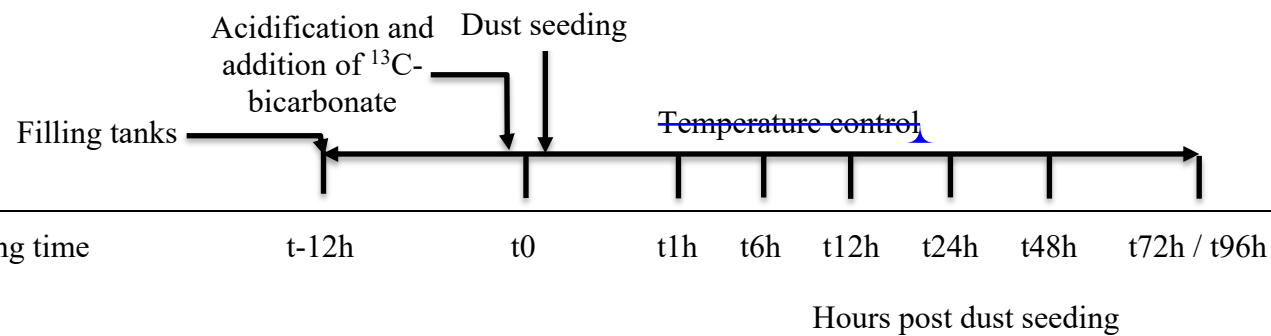


1239 photosynthetic nanoplankton, *Limnology and Oceanography*, 37(7), 1434–1446,  
1240 <https://doi.org/10.4319/lo.1992.37.7.1434>, 1992.

1241 Vidussi, F., Claustre, H., Manca, B. B., Luchetta, A. and Marty, J.-C.: Phytoplankton pigment  
1242 distribution in relation to upper thermocline circulation in the eastern Mediterranean Sea  
1243 during winter, *Journal of Geophysical Research: Oceans*, 106(C9), 19939–19956,  
1244 <https://doi.org/10.1029/1999JC000308>, 2001.

1245

1246 Table 1. List of parameters and processes investigated during the three experiments at stations  
 1247 TYR, ION and FAST. ~~Related~~ manuscripts are indicated.  $pH_T$ : pH on the total scale,  $A_T$ : total  
 1248 alkalinity,  $^{13}C-C_T$ :  $^{13}C$  signature of dissolved inorganic carbon,  $NO_x$ : nitrate + nitrite, DIP:  
 1249 dissolved inorganic phosphorus,  $Si(OH)_4$ : silicate, DFe: dissolved iron, DA1: dissolved  
 1250 aluminium, Th-REE-Pa: Thorium ( $^{230}Th$  and  $^{232}Th$ ), Rare Earth elements and Protactinium  
 1251 ( $^{231}Pa$ ), POC: particulate organic carbon, DOC: dissolved organic carbon,  $^{13}C-DOC$ :  $^{13}C$   
 1252 signature of dissolved organic carbon, TEP: transparent exopolymer particles, NCP/CR: net  
 1253 community production and community respiration (oxygen based),  $^{14}C-PP$ : primary production  
 1254 based on  $^{14}C$  incorporation.



		Related manuscript
Temperature	Continuous	This manuscript
Irradiance	Continuous	This manuscript

**Carbonate chemistry**

pH<sub>T</sub>



This manuscript

A<sub>T</sub>



This manuscript

δ<sup>13</sup>C-C<sub>T</sub>



Gazeau et al. (2021)

**Macro-nutrients**

NO<sub>x</sub>



This manuscript

DIP



This manuscript

Si(OH)<sub>4</sub>



This manuscript

**Micro-nutrients**

DFe



Roy-Barman et al. (2020)

DAI



Roy-Barman et al. (2020)

Th-REE-Pa



Roy-Barman et al. (2020)

**Biological stocks**

Pigments



This manuscript

Flow cytometry



This manuscript

Microscopy				This manuscript
Diazotroph abundance				Céline Ridame (unpublished)
Virus abundance				Dinasquet et al. (2021)
Meta-transcriptomics				Dinasquet et al. (2021)
Bacterial diversity				Dinasquet et al. (2021)
Micro-eukaryote diversity				Dinasquet et al. (2021)
Meso-zooplankton				This manuscript
POC (incl. $\delta^{13}\text{C}$ )				Gazeau et al. (2021)
POC sediment traps				Gazeau et al. (2021)
DOC				Gazeau et al. (2021)
$^{13}\text{C}$ -DOC				Gazeau et al. (2021)
TEP				Gazeau et al. (2021)
Amino acids				Gazeau et al. (2021)
Carbohydrates				Gazeau et al. (2021)
<b>Processes</b>				

NCP/CR

<sup>14</sup>C-PP

~~Plankton~~  
Heterotrophic

Ectoenzymatic activity

N<sub>2</sub> fixation

<sup>13</sup>CO<sub>2</sub>-fixation

Virus production,  
lysogeny

Gazeau et al. (2021)

Gazeau et al. (2021)

Gazeau et al. (2021)

Gazeau et al. (2021)

Céline Ridame (unpublished)

~~Céline Ridame (unpublished)~~  
Gazeau et al. (2021?)

Dinasquet et al. (2021)

1259 Table 2. Initial conditions ~~as measured while filling the tanks (initial conditions in pumped~~  
1260 ~~surface water; sampling time: t-12h).~~ pH<sub>T</sub>: pH on the total scale, NO<sub>x</sub>: nitrate + nitrite, NH<sub>4</sub>:  
1261 ammonium, DIP: dissolved inorganic phosphorus, Si(OH)<sub>4</sub>: silicate, TChl*a*: total chlorophyll *a*,  
1262 HNF: heterotrophic nanoflagellates. The three most important pigments in terms of concentration  
1263 are also presented (19'-hexanoyloxyfucoxanthin, Zeaxanthin and Divinyl Chlorophyll *a*).  
1264 Biomasses of the different groups analyzed through flow cytometry were estimated based on  
1265 conversion equations and/or factors found in the literature (see section 2.3). Autotrophic biomass  
1266 ~~was, as a first approximation, estimated only based on flow cytometry data and therefore~~  
1267 ~~corresponds to the fraction < 20 μm. Heterotrophic biomass was estimated as the sum of~~  
1268 ~~heterotrophic prokaryote and HNF biomasses (see section 2.3.2).~~ Values below detection limits  
1269 are indicated as < dl.

Sampling station	TYR	ION	FAST
Coordinates (decimal)	39.34 N, 12.60 E	35.49 N, 19.78 E	37.95 N, 2.90 N
Bottom depth (m)	3395	3054	2775
Day and time of sampling (local time)	17/05/2017 17:00	25/05/2017 17:00	02/06/2017 21:00
Temperature (°C)	20.6	21.2	21.5
Salinity	37.96	39.02	37.07
Carbonate pH <sub>T</sub>	8.04	8.07	8.03

chemistry	Total alkalinity ( $\mu\text{mol kg}^{-1}$ )	2529	2627	2443
Nutrients	$\text{NO}_x$ ( $\text{nmol L}^{-1}$ )	14.0	18.0	59.0
	$\text{NH}_4^+$ ( $\mu\text{mol L}^{-1}$ )	0.045	0.022	< dl
	DIP ( $\text{nmol L}^{-1}$ )	17.1	6.5	12.9
	$\text{Si(OH)}_4$ ( $\mu\text{mol L}^{-1}$ )	1.0	0.96	0.64
	$\text{NO}_x/\text{DIP}$ (molar ratio)	0.8	2.5	4.6
	Pigments	TChl <i>a</i> ( $\mu\text{g L}^{-1}$ )	0.063	0.066
19'-hexanoyloxyfucoxanthin ( $\mu\text{g L}^{-1}$ )		0.017	0.021	0.016
Zeaxanthin ( $\mu\text{g L}^{-1}$ )		0.009	0.006	0.036
Divinyl Chlorophyll <i>a</i> ( $\mu\text{g L}^{-1}$ )		~ 0	0	0.014
Flow cytometry	Pico-eukaryotes (abundance in cell $\text{mL}^{-1}$ ; biomass in $\mu\text{g C L}^{-1}$ )	347.8; 0.5	239.9; 0.4	701.0; 1.0
	Nano-eukaryotes (abundance in cell $\text{mL}^{-1}$ ; biomass in $\mu\text{g C L}^{-1}$ )	150.5; 3.9	188.8; 4.8	196.6; 5.0
	<i>Synechococcus</i> (abundance in cell $\text{mL}^{-1}$ ; biomass in $\mu\text{g C L}^{-1}$ )	4972; 1.2	3037; 0.8	6406; 1.6
	Autotrophic biomass ( $\mu\text{g C L}^{-1}$ )	5.6	6.0	7.7
	Heterotrophic prokaryotes abundance ( $\times 10^5$ cell $\text{mL}^{-1}$ )	4.79	2.14	6.15
	HNF (abundance in cell $\text{mL}^{-1}$ )	110.1	53.6	126.2
	Heterotrophic biomass ( $\mu\text{g C L}^{-1}$ )	9.9	4.5	12.7
Microscopy	Pennate diatoms (abundance in cell $\text{L}^{-1}$ )	140	520	880
	Centric diatoms (abundance in cell $\text{L}^{-1}$ )	200	380	580

Dinoflagellates (abundance in cell L <sup>-1</sup> )	2770	3000	3410
Autotrophic flagellates (abundance in cell L <sup>-1</sup> )	0	60	650
Ciliates (abundance in cell L <sup>-1</sup> )	270	380	770

---



Table 3. Maximum input of nitrate + nitrite (NO<sub>x</sub>) and dissolved inorganic phosphorus (DIP) released from Saharan dust in tanks D and G as observed from the ~~two~~ discrete samplings ~~performed over~~ the first 6 h after seeding. The estimated maximal percentage of dissolution is also presented (see section 2.3.1 for details on the calculations).

	NO <sub>x</sub>				DIP			
	D1	D2	G1	G2	D1	D2	G1	G2
Maximum input	μmol L <sup>-1</sup>				nmol L <sup>-1</sup>			
TYR	11.0	11.1	11.1	11.0	24.6	20.4	24.6	23.9
ION	11.2	11.6	11.2	11.3	23.3	22.0	19.6	22.9
FAST	11.3	11.1	11.1	11.2	30.8	31.3	36.9	29.8
Percentage of dissolution (%)								
TYR	95	96	95	94	12	10	12	11
ION	96	99	96	97	11	10	9	11
FAST	97	97	95	97	15	15	17	14

1 Table 4. Removal rate of nitrate + nitrite (NO<sub>x</sub>) and dissolved inorganic phosphorus (DIP) in  
 2 tanks D and G during the three experiments (TYR, ION and FAST). For NO<sub>x</sub>, ~~decreasing~~  
 3 were estimated based on linear regressions between maximal concentrations (i.e. after dust  
 4 enrichment, at t1h or t6h) and final concentrations (t72 h for TYR and ION and t96h for FAST).  
 5 For DIP, ~~decreasing~~ rates were estimated based on linear regressions between maximal  
 6 concentrations (i.e. after dust enrichment at t1h or t6h) and concentrations ~~measured at sampling~~  
 7 ~~times after which a~~ stabilization was observed. This sampling time is shown in parentheses. All  
 8 rates are expressed in nmol L<sup>-1</sup> h<sup>-1</sup>.

	NO <sub>x</sub>			DIP		
	TYR	ION	FAST	TYR	ION	FAST
D1	-6.5	-8.6	-14.3	-0.4 (t72h)	-0.5 (t48h)	-0.2 (t96h)
D2	-1.0	-8.6	-13.5	-0.3 (t72h)	-0.8 (t24h)	-0.2 (t96h)
G1	-6.7	-13.1	-21.6	-1.3 (t24h)	-0.8 (t24h)	-1.5 (t24h)
G2	-0.8	-1.6	-25.2	-1.3 (t24h)	-1.6 (t24h)	-1.1 (t24h)

10 Table 5. Maximum relative changes in tanks D and G as compared to controls (average between  
 11 C1 and C2), ~~expressed as a %, for the three experiments (TYR, ION and FAST)~~. The sampling  
 12 time at which these maximum relative changes were observed is shown in brackets. Tchl $a$  refers  
 13 to the concentration of total chlorophyll  $a$  and B $_{micro}$  to the biomass proxy of micro-  
 14 phytoplankton (sum of Fucoxanthin and Peridinin, see Material and Methods) based on high  
 15 performance liquid chromatography (HPLC). HP and HNF refer to heterotrophic prokaryote and  
 16 heterotrophic nanoflagellate abundances, respectively, ~~as~~ measured by flow cytometry.

Experiment	Tank	HPLC		Flow cytometry				
		TChl $a$	B $_{micro}$	Pico-eukaryotes	Nano-eukaryotes	<i>Synechococcus</i>	HP	HNF
TYR	D1	-35 (t24h)	-33 (t12h)	-75 (t72h)	-80 (t1h)	-71 (t48h)	68 (t72h)	352 (t72h)
TYR	D2	-38 (t12h)	-39 (t24h)	-75 (t72h)	-80 (t1h)	-72 (t48h)	53 (t72h)	100 (t72h)
TYR	G1	60 (t72h)	52 (t72h)	-75 (t1h)	89 (t72h)	76 (t72h)	67 (t72h)	1095 (t72h)
TYR	G2	359 (t72h)	392 (t72h)	323 (t72h)	119 (t72h)	700 (t72h)	68 (t48h)	298 (t72h)
ION	D1	183 (t72h)	157 (t72h)	126 (t72h)	89 (t72h)	317 (t72h)	128 (t72h)	44 (t72h)
ION	D2	109 (t72h)	156 (t72h)	117 (t72h)	-59 (t1h)	390 (t72h)	133 (t72h)	27 (t72h)
ION	G1	399 (t72h)	454 (t72h)	458 (t72h)	256 (t72h)	805 (t72h)	176 (t72h)	175 (t72h)

ION	G2	426 (t72h)	612 (t72h)	510 (t72h)	292 (t72h)	1425 (t72h)	161 (t72h)	129 (t72h)
FAST	D1	318 (t96h)	356 (t96h)	113 (t96h)	208 (t72h)	348 (t96h)	27 (t96h)	-38 (t96h)
FAST	D2	237 (t96h)	322 (t96h)	91 (t96h)	219 (t72h)	197 (t96h)	40 (t48h)	-49 (t96h)
FAST	G1	399 (t96h)	415 (t96h)	198 (t72h)	274 (t72h)	357 (t48h)	61 (t48h)	243 (t24h)
FAST	G2	395 (t96h)	421 (t96h)	129 (t72h)	202 (t96h)	344 (t48h)	67 (t48h)	74 (t24h)

---

## Figure captions

Fig. 1. Location of the sampling stations in the Mediterranean Sea onboard the R/V “Pourquoi Pas ?” during the PEACETIME cruise, ~~on map of~~ satellite-derived surface chlorophyll *a* concentration averaged over the entire duration of the cruise (Courtesy of Louise Rousselet).

Fig. 2. ~~Scheme~~ of an experimental tank (climate reactor).

Fig. 3. Proportion of the different pigments, as measured by high performance liquid chromatography (HPLC) in pumped surface seawater for the three experiments (t-12h).

Fig. 4. Continuous measurements of temperature and irradiance level (PAR) in the six tanks during the ~~three~~ experiments. The dashed vertical line indicates the time of dust seeding (after  $t_0$ ).

Fig. 5. pH on the total scale ( $\text{pH}_T$ ) and total alkalinity ( $A_T$ ) measured in the six tanks during the ~~three~~ experiments. The dashed vertical line indicates the time of dust seeding (after  $t_0$ ). Error bars correspond to the standard deviation based on analytical triplicates.

Fig. 6. Nutrients (nitrate + nitrite:  $\text{NO}_x$ , dissolved inorganic phosphorus: DIP, silicate:  $\text{Si}(\text{OH})_4$  ~~as well as the~~ molar ratio between  $\text{NO}_x$  and DIP, measured in ~~the six~~ tanks during the ~~three~~ experiments. The dashed vertical line indicates the time of seeding (after  $t_0$ ).

Fig. 7. ~~Concentrations of~~ total chlorophyll *a* and major pigments, ~~measured by~~ high performance liquid chromatography (HPLC), in ~~the six~~ tanks during the ~~three~~ experiments. The dashed vertical line indicates the time of seeding (after  $t_0$ ).

Fig. 8. Abundance of autotrophic pico-eukaryotes, autotrophic nano-eukaryotes, *Synechococcus*, heterotrophic prokaryotes (HP), and heterotrophic nano-flagellates (HNF), measured by flow cytometry, in the ~~six~~ tanks during the ~~three~~ experiments. The evolution of autotrophic biomass

(see Material and Methods for details on the calculation) is also shown. The dashed vertical line indicates the time of seeding (after  $t_0$ ).

Fig. 9. Abundances of meso-zooplankton species as measured at the end of each experiment.

Fig. 10. Maximal relative change (%) of main biological stocks (TCHl $a$ : total chlorophyll  $a$ , HP: heterotrophic prokaryotes) and processes (BP: bacterial production; PP:  $^{14}\text{C}$ -based primary production; see Gazeau et al., 2021; BR: bacterial respiration (no data from this study); and  $\text{N}_2$  fixation, Céline Ridame, unpublished results) as obtained during the present study at the 3 stations (TYR, ION and FAST) under ambient conditions of pH and temperature (open red squares) and future conditions (full green squares). Squares are delimited by the range of responses observed among the duplicates for each treatment. The dotted green squares for station TYR denote the large variability observed between duplicates for some parameters and processes that prevented drawing solid conclusions. Box-plots represent the distribution of responses observed from studies conducted in the Mediterranean Sea, as compiled by Guieu and Ridame (2020).

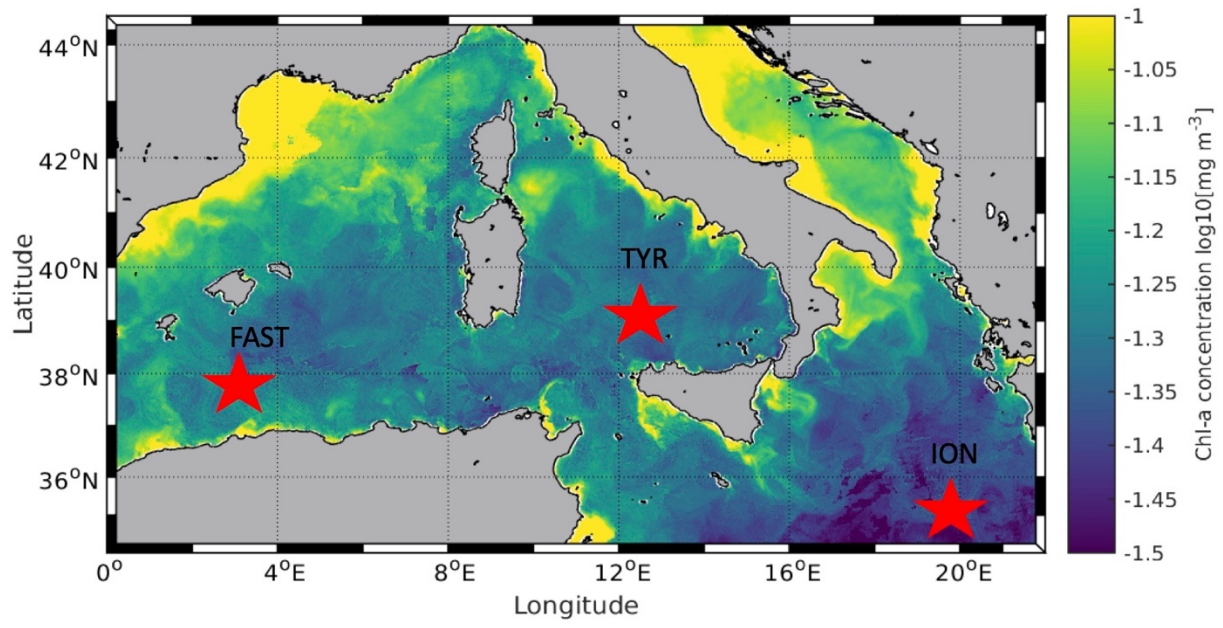


Fig. 1.

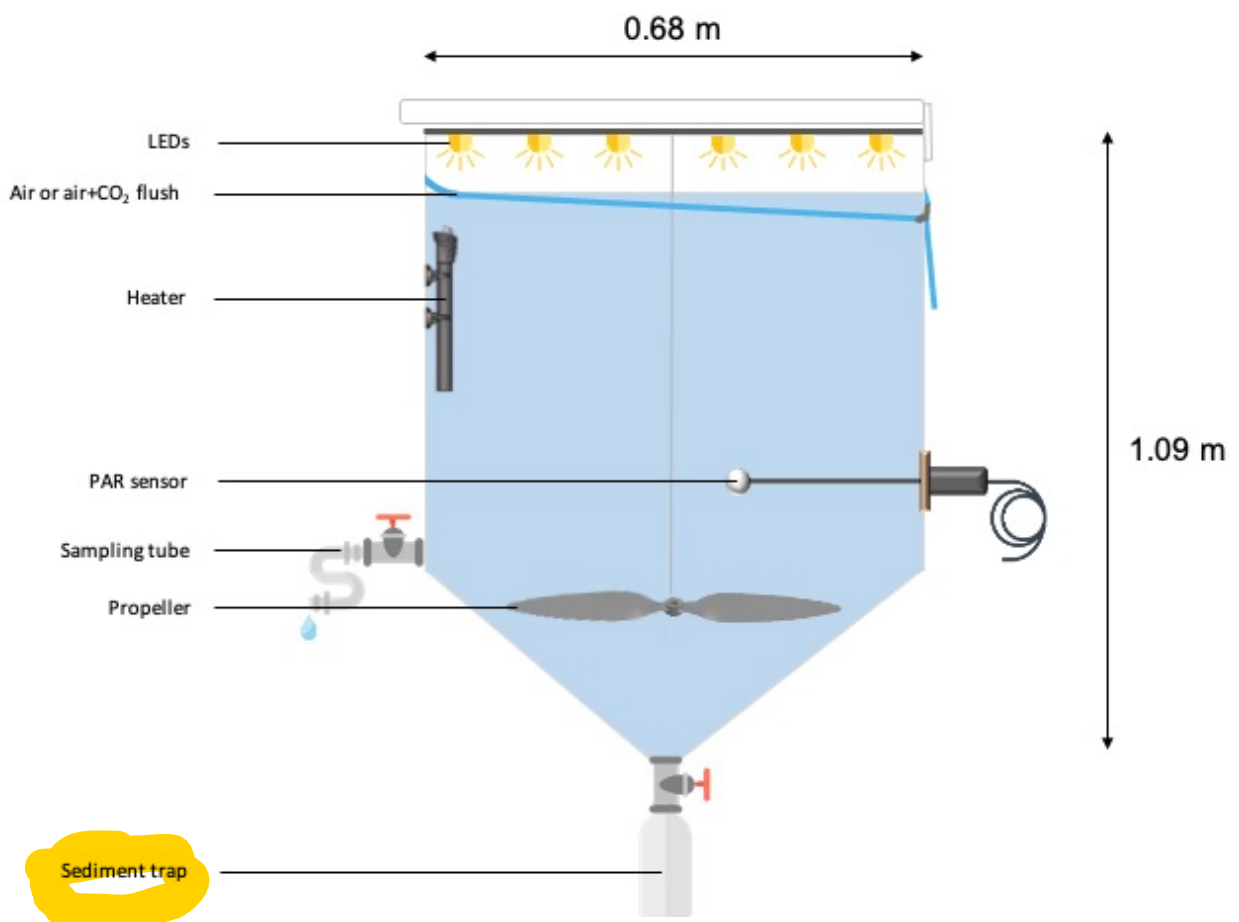


Fig. 2.



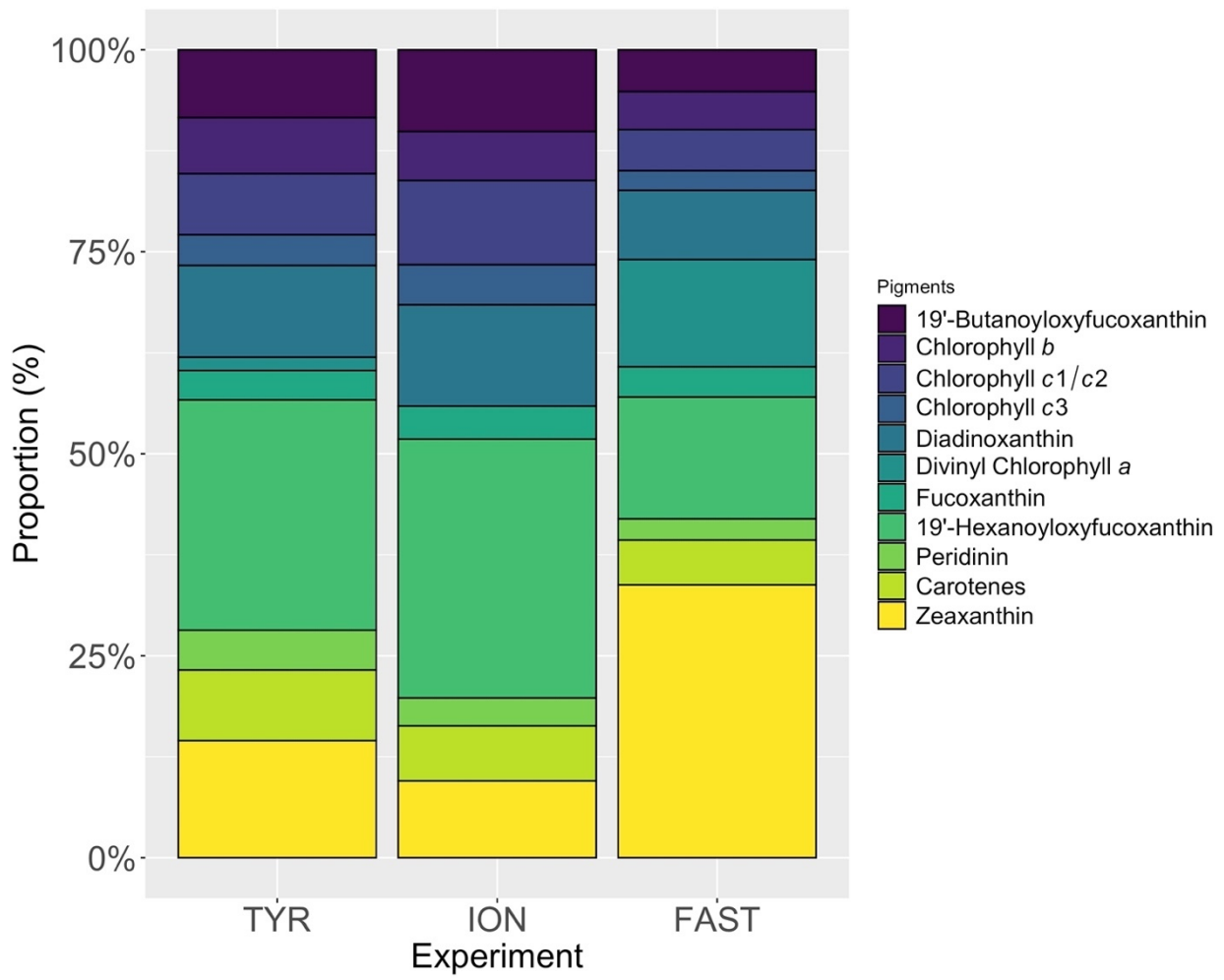


Fig. 3.

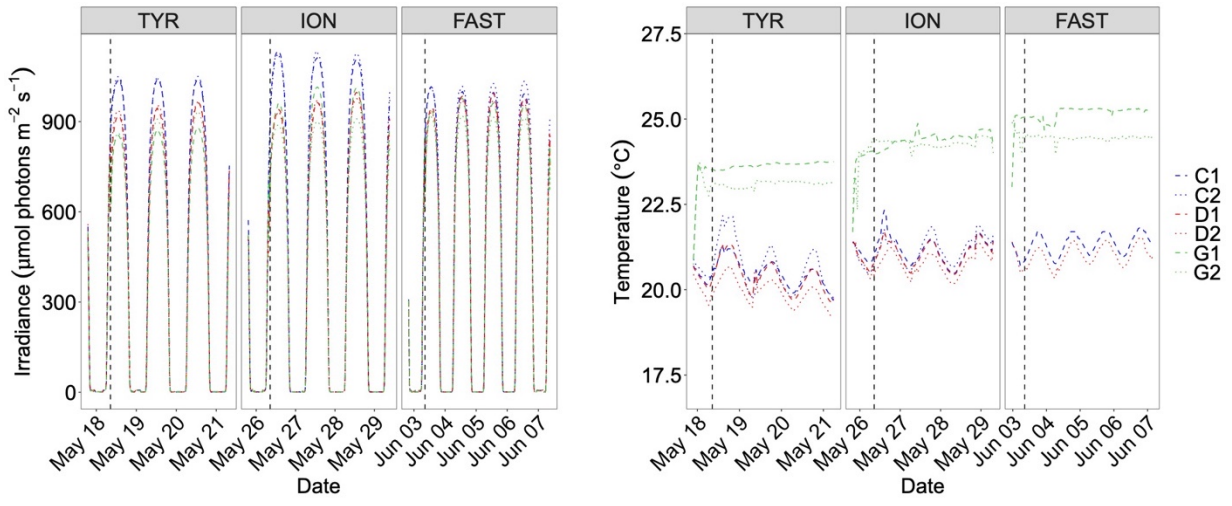


Fig. 4.

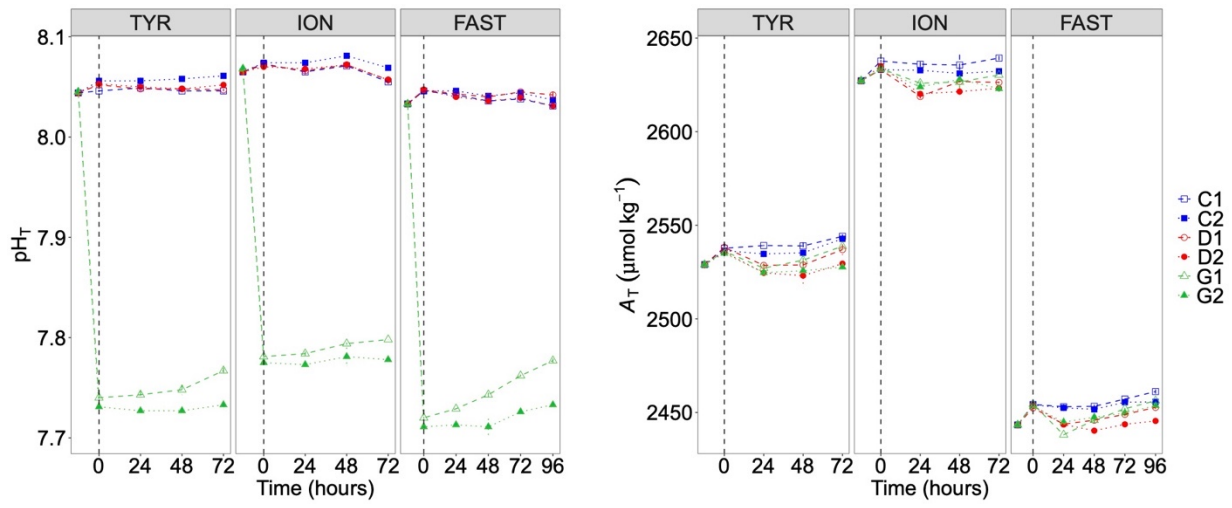


Fig. 5.

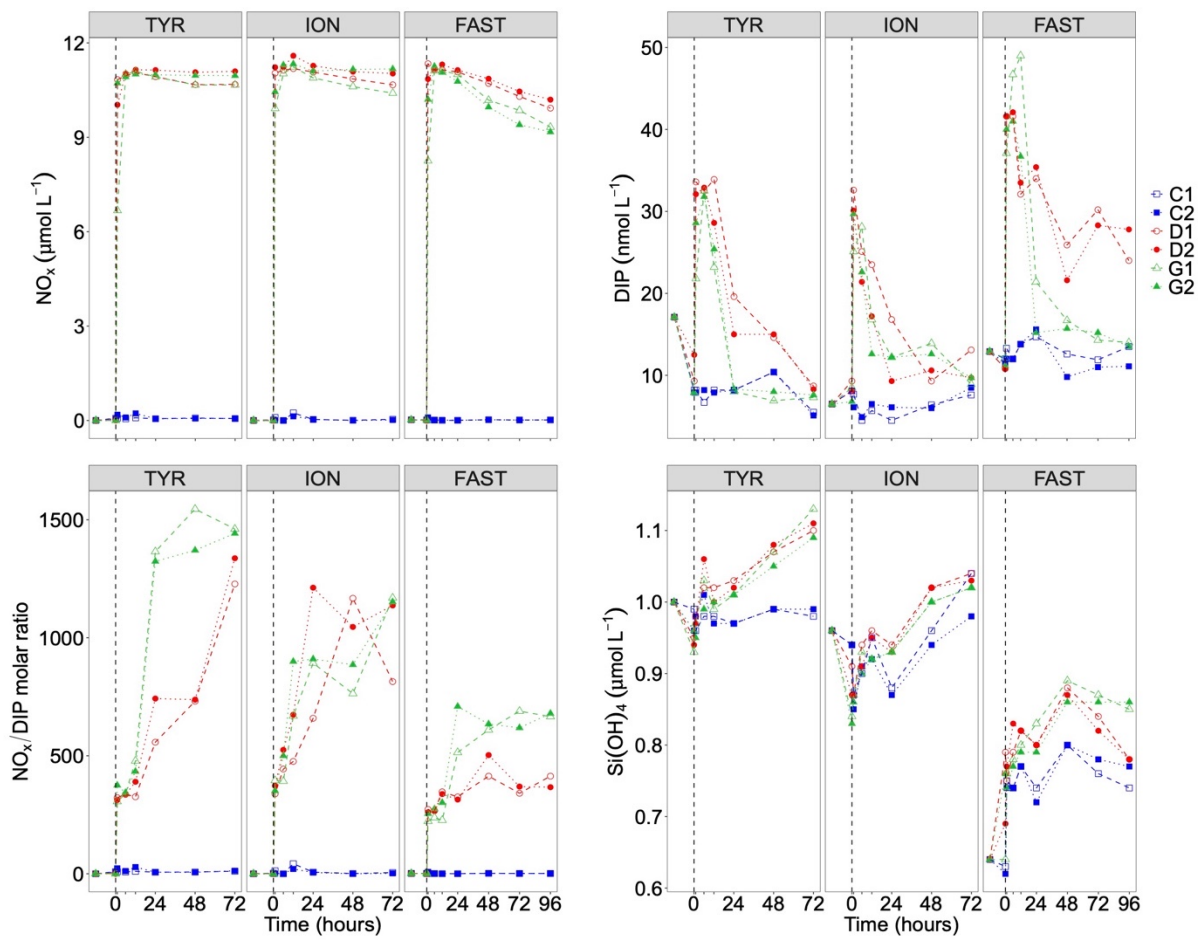


Fig. 6.

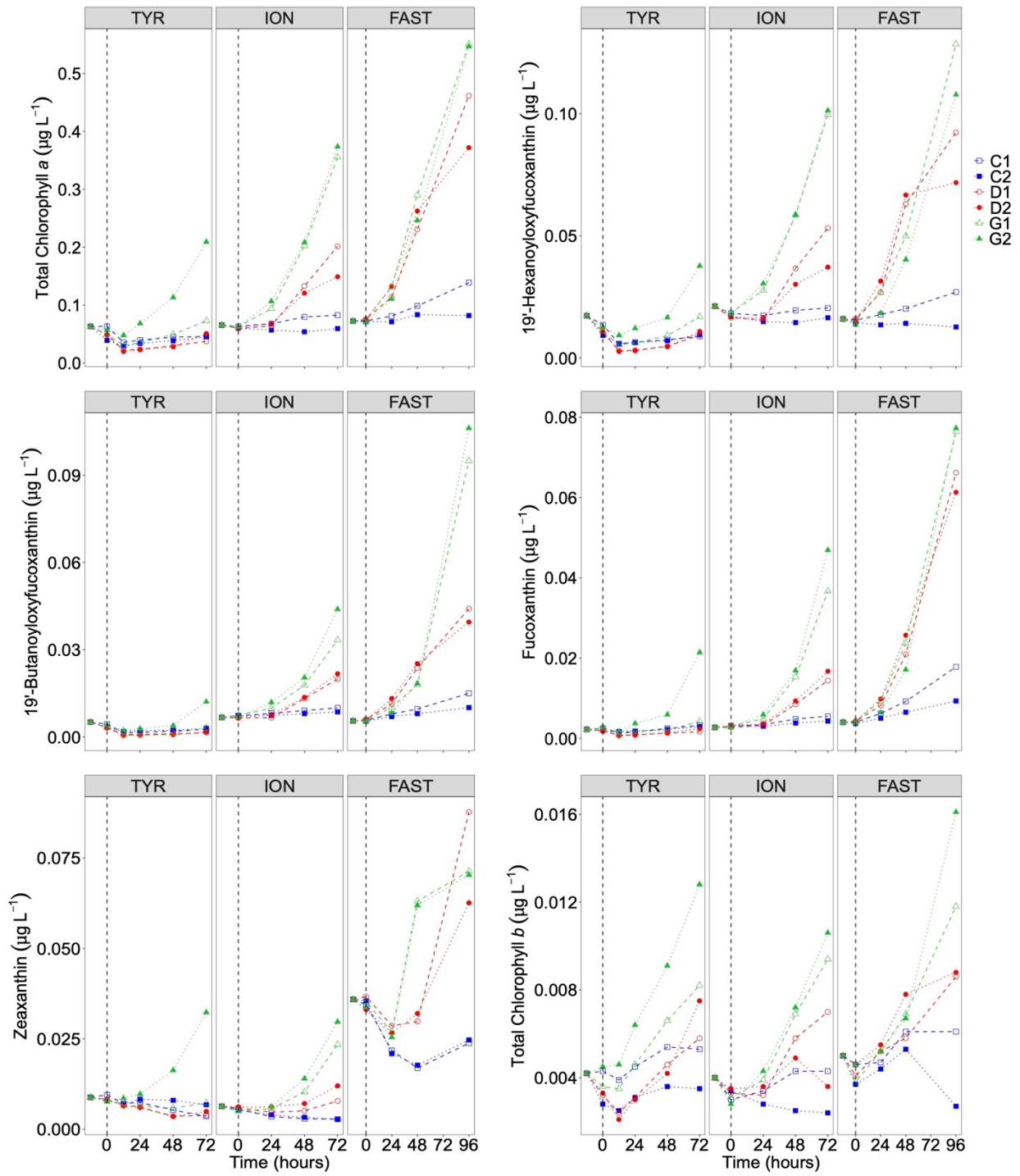


Fig. 7.

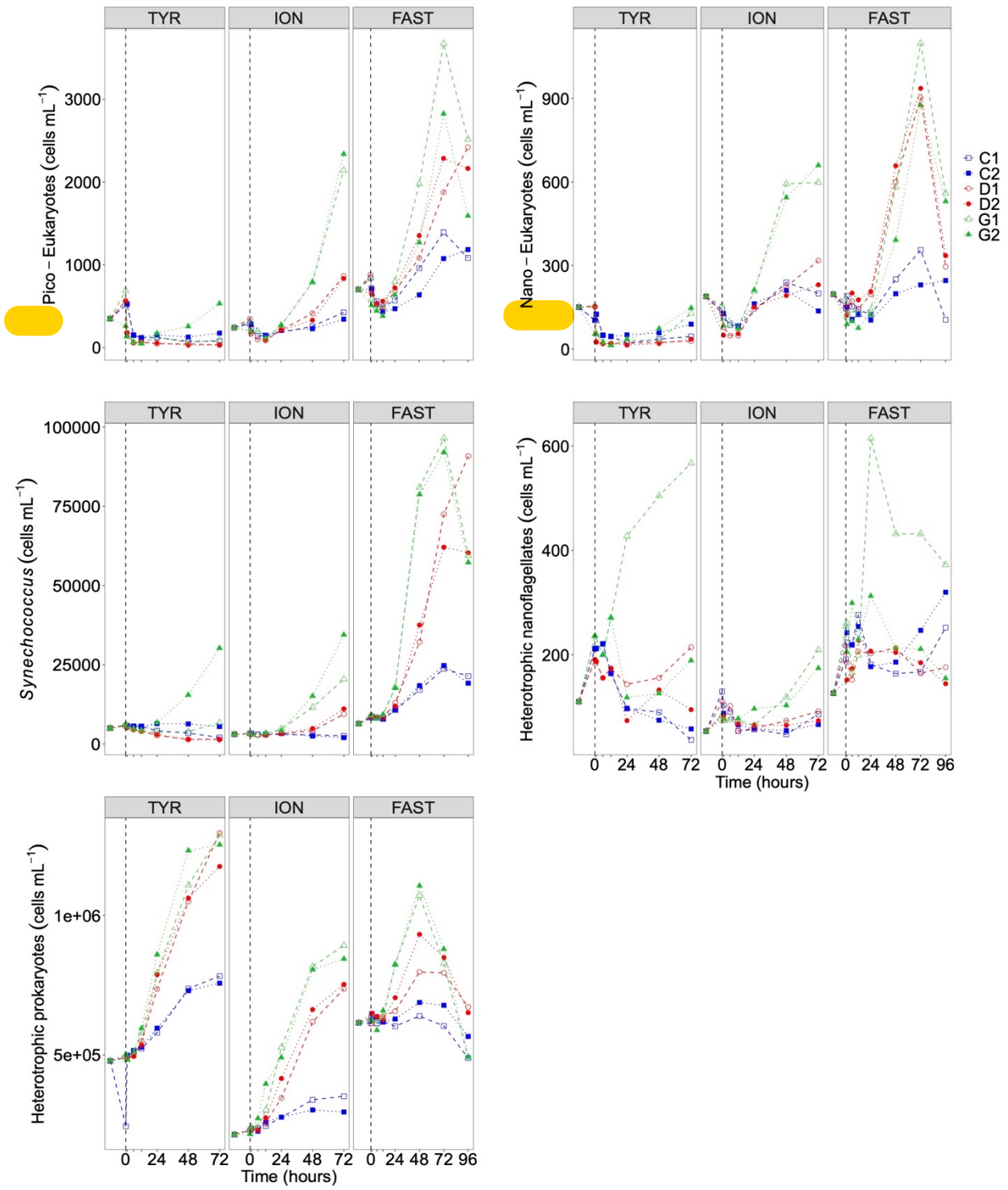


Fig. 8.

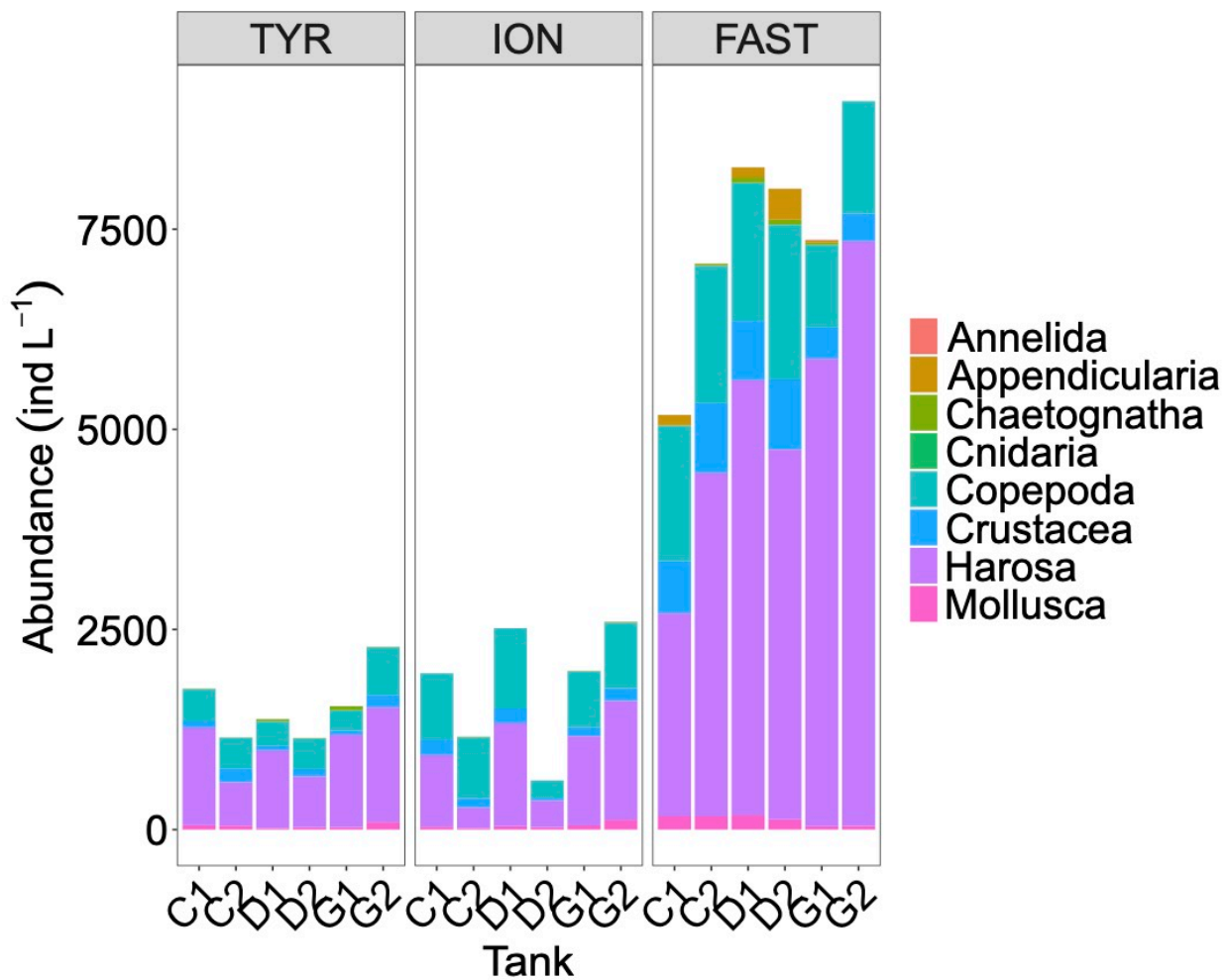


Fig. 9.

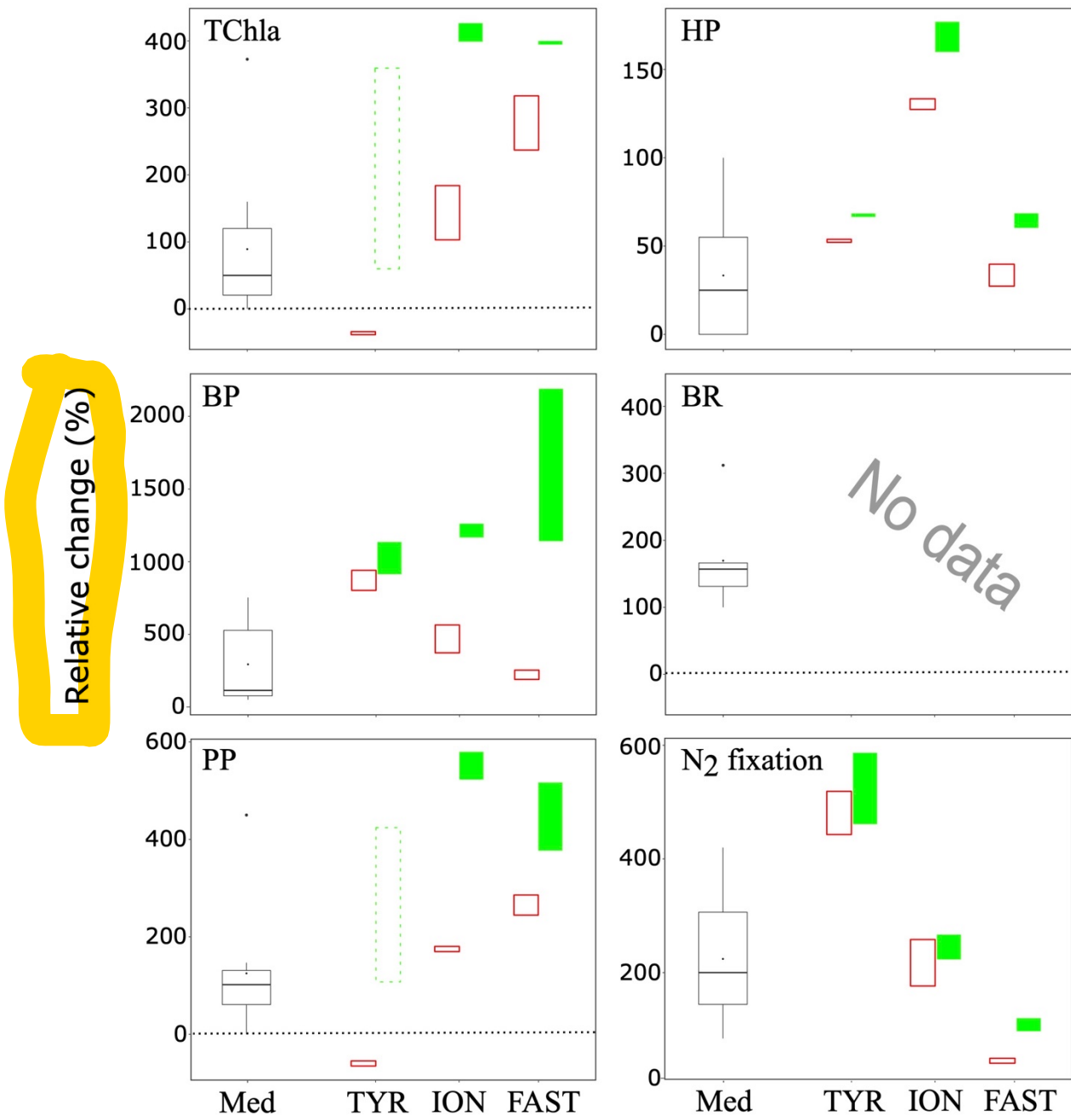


Fig. 10.